OCEAN DRILLING PROGRAM

LEG 197 SCIENTIFIC PROSPECTUS

MOTION OF THE HAWAIIAN HOTSPOT: A PALEOMAGNETIC TEST

Dr. Robert A. Duncan
Co-Chief Scientist
Oregon State University
College of Oceanic and Atmospheric Sciences
104 Ocean Administration Building
Corvallis OR 97331-5503
USA

Dr. John A. Tarduno
Co-Chief Scientist
University of Rochester
Department of Earth and
Environmental Sciences
Hutchison Hall 227
Rochester NY 14627
USA

Dr. Jack Baldauf
Deputy Director of Science Operations
Ocean Drilling Program
Texas A&M University
1000 Discovery Drive
College Station TX 77845-9547
USA

Dr. Gary D. Acton
Leg Project Manager and Staff Scientist
Ocean Drilling Program
Texas A&M University
1000 Discovery Drive
College Station TX 77845-9547
USA

May 2001

Ocean Drilling Program Scientific Prospectus No. 97 (May 2001)

Distribution: Electronic copies of this publication may be obtained from the ODP Publications homepage on the World Wide Web at: http://www-odp.tamu.edu/publications

This publication was prepared by the Ocean Drilling Program, Texas A&M University, as an account of work performed under the international Ocean Drilling Program, which is managed by Joint Oceanographic Institutions, Inc., under contract with the National Science Foundation. Funding for the program is provided by the following agencies:

Australia/Canada/Chinese Taipei/Korea Consortium for Ocean Drilling
Deutsche Forschungsgemeinschaft (Federal Republic of Germany)
Institut National des Sciences de l'Univers-Centre National de la Recherche Scientifique (INSU CNRS; France)
Ocean Research Institute of the University of Tokyo (Japan)
National Science Foundation (United States)
Natural Environment Research Council (United Kingdom)
European Science Foundation Consortium for Ocean Drilling (Belgium, Denmark, Finland, Iceland, Ireland, Italy, The Netherlands, Norway, Portugal, Spain, Sweden, and Switzerland)
Marine High-Technology Bureau of the State Science and Technology Commission of the People's Republic of China

This Scientific Prospectus is based on precruise JOIDES panel discussions and scientific input from the designated Co-Chief Scientists on behalf of the drilling proponents. The operational plans within reflect JOIDES Planning Committee and thematic panel priorities. During the course of the cruise, actual site operations may indicate to the Co-Chief Scientists and the Operations Manager that it would be scientifically or operationally advantageous to amend the plan detailed in this prospectus. It should be understood that any proposed changes to the plan presented here are contingent upon approval of the Director of the Ocean Drilling Program in consultation with the Science and Operations Committees (successors to the Planning Committee) and the Pollution Prevention and Safety Panel.

Technical Editors: Karen K. Graber and Lorri L. Peters

ABSTRACT

The bend in the Hawaiian-Emperor chain is the best example of a change in plate motion recorded in a fixed-hotspot frame of reference. Alternatively, the bend might primarily record differences in motion of the Hawaiian hotspot relative to the Pacific lithosphere. Four lines of inquiry support the latter view: (1) global plate motions predicted from relative plate motion data, (2) spreading rate data from the North Pacific basin, (3) mantle flow modeling utilizing geoid and seismic tomography constraints, and (4) new paleomagnetic data from the Emperor chain. Although the rate of motion is difficult to constrain because previous drilling has been limited, the best available paleomagnetic data suggest Pacific hotspots may have moved at rates comparable to those of lithospheric plates in Late Cretaceous to early Tertiary times (81-43 Ma). If correct, this requires a major change in how we view mantle dynamics and the history of plate motions. This leg seeks to test the hypothesis of southward motion of the Hawaiian hotspot by drilling five to six basement sites in the Emperor seamount trend. The principal drilling objective is to achieve moderate basement penetration (150-250 m) at these sites to obtain cores from lava flows suitable for paleomagnetic paleolatitude and radiometric age determinations. A comparison of these dated paleolatitude values with fixed and moving hotspot predictions form the basis of the proposed test. Our sampling strategy will also allow us to address important geomagnetic questions that require paleomagnetic data from the Pacific plate, including the history of the time-average field and its paleointensity. The data obtained will place fundamental constraints on the Late Cretaceous to early Tertiary motion of the Pacific plate. An improved picture of this motion history is needed if proxy climatic data from previous and future drill sites are to be used to define past latitudinal gradients.

Another important science objective is to determine the geochemical variation of the volcanic products of the Hawaiian hotspot through time. Petrologic and compositional data from cored lava flows will be used to document changes in source and melting conditions (temperature, depth, and extent) over the duration of Emperor seamount formation. The effect of proposed changes in plate setting (near spreading ridge to mid-plate with decreasing age) on magma composition will be evaluated. The well-known stages of Hawaiian island formation (tholeiitic shield, alkalic capping, and post-erosional flows) will be used to assess lava flow compositions in the context of volcano development. Alteration studies will provide estimates of elemental fluxes in submarine or subaerial weathering conditions. Finally, cored lava flows will be examined with regard to the physical volcanology of these Emperor seamounts. Estimates of size and frequency of eruptions and

distance from source will be based on the characteristics of Hawaiian island flows (e.g., morphology, vesicularity, and crystallinity).

INTRODUCTION

Many of our ideas on where mantle plumes originate, how they interact with the convecting mantle, and how plates have moved in the past rest on interpretations of the Hawaiian-Emperor hotspot track. One reason this volcanic lineament has attained this conceptual stature lies in its prominent bend at 43 Ma. The bend, which separates the westward trending Hawaiian islands from the northward trending Emperor seamounts (Fig. 1), has no equal among the Earth's hotspot tracks. It is the clearest physical manifestation of a change in plate motion in a fixed hotspot reference frame. Because the bend is so distinct, it can be used to estimate plume diameters and to place bounds on the velocity and viscosity of the convecting upper mantle that may deflect plumes (Duncan and Richards, 1991). However, shortly after hotspots were used as a frame of reference (Morgan, 1971), apparent discrepancies involving the Hawaiian-Emperor track arose (Molnar and Atwater, 1973). Attempts to model past plate motions failed to predict the bend; instead, a more westerly track was derived (Solomon et al., 1977). Tests of the fixed hotspot hypothesis suggested large relative motions between Hawaii and hotspots in the Atlantic and Indian Ocean basins (Molnar and Atwater, 1973; Molnar and Stock, 1987), but uncertainties in the plate circuits employed in these tests limited their resolving power (Acton and Gordon, 1994).

Recently, several works have readdressed these questions. Norton (1995) suggested that the Hawaiian-Emperor bend records the time when the hotspot became fixed in the mantle. Prior to 43 Ma, according to Norton (1995), the hotspot moved southward, creating the Emperor seamount chain. This work is difficult to assess because of the lack of formal error analyses, but the interpretation reiterates findings of updated plate circuit studies that consider rotation pole errors (Cande et al, 1995). In addition, there is no obvious change in spreading rate at 43 Ma in the well-studied marine magnetic anomaly record of the North Pacific (Atwater, 1989). Many feel the lack of such a response by neighboring plates to a change in Pacific plate motion as large as that indicated by the Hawaiian-Emperor bend is reason enough to question hotspot fixity. New modeling efforts, utilizing a viscosity structure based on geoid constraints, mantle flow fields consistent with tomographic data, and plate motion estimates also predict motion of hotspot groups (Steinberger

and O'Connell, 1997). For the Emperor trend, the predicted motion is 10-15 mm/yr (Steinberger, 1996) (Fig. 2).

Whereas these recent studies have revitalized discussions regarding hotspot fixity (see also Christensen, 1998; Wessel and Kroenke, 1998), they face some fundamental data limitations. Fortunately, the hypothesis of hotspot motion can be tested independently using paleomagnetic data. If the hotspot has remained fixed (with respect to Earth's spin axis), the paleolatitudes of extinct volcanic edifices comprising the Emperor chain should match the present-day latitude of Hawaii but these tests are difficult in practice. For example, paleomagnetic data from some deep-sea sediments show a bias caused by compaction-induced flattening (Tarduno, 1990). Such problems can be avoided through the study of drill cores from well-dated lava flows. Until recently, however, only a few sites had sufficient depth penetration. This situation has improved with the latest Pacific drilling. Data from Ocean Drilling Program (ODP) Legs 143 and 144 indicate significant motions between hotspot groups in the Atlantic and Pacific Oceans during the mid-Cretaceous (128-95 Ma) (Tarduno and Gee, 1995). The motion is rapid, at speeds typical of lithospheric plates (30 mm/yr).

These findings indicate an older episode of hotspot motion and, coupled with the inferences based on relative plate motions, suggest that Hawaiian hotspot motion is a viable hypothesis that should be tested further. New data obtained from the Emperor chain drilled during Leg 145 have allowed a preliminary test. Below we summarize these analyses (Tarduno and Cottrell, 1997), as they provide support for the hypothesis and have guided our proposed sampling plan. In addition, we outline how sites chosen to address the question of hotspot fixity can provide crucial data required for understanding characteristics of the past geomagnetic field and for determining the compositional variability of volcanic products from the Hawaiian hotspot.

BACKGROUND AND RECENT RESULTS

Paleomagnetic Bias in Sedimentary Inclinations

One potential way to address the question of hotspot fixity is to obtain paleomagnetic data from deep-sea sediments. The advantages of this approach are clear: at a given site well-dated sediments might allow a nearly continuous latitudinal record of plate motion. By combining data from several distant sites, paleomagnetic poles can be constructed, yielding an apparent polar wander path.

Paleomagnetic data from sediments are available from numerous Pacific Deep Sea Drilling Project (DSDP) and ODP sites. These data can be examined to test whether they define an internally consistent picture of plate motion (Fig. 3). Unfortunately, the data are systematically shallower than coeval inclination values derived from igneous sources (e.g., Gordon, 1990). The differences are consistent with compaction-induced inclination shallowing (Tarduno, 1990; Butler, 1992). Sediments can acquire a detrital magnetization when magnetic grains orient in the presence of the Earth's geomagnetic field. A flattening of inclination, however, is well documented for certain sediment types, especially glacial varves. The error is described as

$$\tan I_o = \mathrm{f} \tan I_e.$$

where I_o is the observed inclination, I_e is the expected inclination, and f is an empirically determined flattening factor. For glacial varves, f = 0.40 has been reported (King, 1955).

It was once thought that the deep-sea sediments might escape the effects of inclination error because their magnetization was thought to be a post-depositional remanent magnetization (pDRM), which was locked in not at the sediment-water interface, but slightly deeper, within an interval where magnetic grains were still free to rotate in pore spaces (Verosub, 1977; deMenocal et al., 1990). Nevertheless, observations from all the world's oceans appeared to define shallow inclinations in some deep-sea sediments (e.g., Celaya and Clement, 1988; Arason and Levi, 1990; Larson et al., 1992) and subsequent experimental results on synthetic samples have confirmed that a pDRM can be shallowed by compaction (Kodama and Sun, 1992; Sun and Kodama, 1992).

The Pacific sedimentary inclination data studies by Tarduno (1990), which are mainly Cretaceous in age, define a f = 0.52. Considerable scatter in this value is not surprising: sediments ranging from carbonates to volcaniclastics were combined and sediment type clearly must play a role in compaction. This calculation also relies on expected inclinations calculated from the sparse, ca. 1990 igneous data set (e.g., basalt colatitudes). Results from subsequent drilling have tended to confirm previous notions of mid-Cretaceous pole positions (Tarduno and Sager, 1995; Tarduno and Gee, 1995). In addition, whereas errors in the reference data (poles) can affect the degree of flattening, the overall distribution remains internally inconsistent and requires inclination shallowing. Any remaining doubt about the mechanism was put to rest by the magnetic anisotropy

work by Hodych and Bijaksana (1993) on the same sites studied in Tarduno (1990). This work documented that the development of a magnetic fabric in Pacific deep-sea sediments was proportional to the flattening values predicted in Tarduno (1990).

The potential problems caused by inclination shallowing are particularly severe in our proposed study for several reasons. The amount of error varies with expected latitude. Because the expected latitude values in the moving hotspot hypothesis range between 40° and 60°, the errors will be at their maximum potential values for flattening values similar to those reported in natural sediments (Fig. 4A). These errors are of the same magnitude as the total inclination offset we seek to test (Fig. 4B). Whereas substantial advances have been made in using magnetic anisotropy to correct for inclination shallowing (e.g., Jackson et al., 1991), the potential errors are, in our opinion, too large for this to yield an unambiguous, high-resolution test of the fixed vs. moving hotspot models.

We note, however, that a few sites in the Pacific, particularly shallow-water sediments (Tarduno and Gee, 1995) have yielded data that do not appear to have suffered significant inclination shallowing. This may be due to relatively early cementation, and similar sediments could be encountered during drilling. However, because it can be difficult to obtain high-resolution age data on some shallow-water sediments and recovery is problematic, they do not provide a viable alternative to basalt drilling.

New Paleolatitude Data for the Emperor Seamounts

During Leg 145, 87 m of lava flows were penetrated on Detroit Seamount (Fig. 1) (Rea, Basov, Scholl, and Allan, 1995). $^{40}Ar/^{39}Ar$ radiometric analyses yield an age (81.2 ± 1.3 Ma [Keller et al., 1995]) older than that assumed in hotspot-based plate-motion models (~75 Ma) (Duncan and Clague, 1985). Characteristic magnetizations derived from basalt samples have mainly negative inclinations indicating reversed polarity (Fig. 1). This polarity assignment is consistent with the radiometric age data, suggesting eruption of the basalts during Chron 33R (79-83 Ma) (Tarduno and Cottrell, 1997).

A potential problem in obtaining reliable paleomagnetic data from any basalt drill hole is the uncertain timescale between eruptions. If most flows reflect rapid eruptions, one could easily obtain a biased paleolatitude estimate by giving equal weight to each flow unit. To address this concern, the inclination-only averages derived from each flow unit (McFadden and Reid, 1982) must be checked

for serial correlation (Cox, 1970; Kono, 1980; Tarduno and Sager, 1995). These analyses lead to inclination-group models (Fig. 5). The directional angular dispersion, estimated from the inclination-model data and transformed into pole space (Cox, 1970; Tarduno and Sager, 1995), is indistinguishable from the predicted virtual geomagnetic pole scatter from global data sets (McFadden et al., 1991) (Fig. 5). As discussed below, there is only one other paleomagnetic data set from the Emperor trend that satisfies these geomagnetic-sampling requirements.

The preferred inclination group model, where groups are distinct at >95% confidence (N = 10) (Kono, 1980), suggests a paleolatitude of 36.2° (+6.9°/-7.2°), clearly discordant from the present-day latitude of Hawaii (~19°) (Fig. 5). This discrepancy is too large to be explained by tectonic tilt. Tilts of 1°-3° have been reported previously for some of the northern Emperor seamounts (Lonsdale et al., 1993). Because these tilts are small and the angle between the remanent magnetization vector and down-dip azimuth of tilt is large (>60°), the effect on the paleolatitude is negligible. Measurements made at unit contacts also fail to indicate significant dips (Tarduno and Cottrell, 1997).

The new paleomagnetic result directly questions the validity of the Late Cretaceous Pacific apparent polar wander path (Fig. 5). But how could these prior results be so errant? Previous Late Cretaceous poles are heavily or solely based on the inversion of magnetic surveys over seamounts (Gordon, 1983; Sager and Pringle, 1988). Reviews of the methods used to fit these poles suggest they are far more uncertain than commonly supposed (Parker, 1991). Viscous and induced magnetizations can also bias the resulting pole positions (Gee et al., 1989). Interestingly, high-latitude poles similar to the new colatitude result (Fig. 5) have been reported from preliminary analyses of marine magnetic anomaly skewness data of comparable age (Vasas et al., 1994).

Hotspot Motion and True Polar Wander

The other paleolatitude value from the Emperor trend that adequately averages secular variation was derived from Suiko Seamount (65 Ma) (Kono, 1980) (Fig. 1). The 8° discrepancy between the Suiko Seamount paleolatitude and the present-day latitude of the Hawaiian islands has been attributed previously to early Cenozoic true polar wander (Gordon and Cape, 1981; Sager and Bleil, 1987), which is defined as a rotation of the entire solid Earth in response to shifting mass heterogeneities in the mantle (Goldreich and Toomre, 1969). True polar wander predictions based

on global paleomagnetic data from the continents (Besse and Courtillot, 1991), however, do not agree with the new Detroit Seamount data (Tarduno and Gee, 1995; Tarduno and Cottrell, 1997). Furthermore, renewed tests of Cretaceous true polar wander models show that the solid Earth rotations proposed are not seen in paleomagnetic data from regions where large changes in latitude should be observed (Cottrell and Tarduno, 2000b; Tarduno and Smirnov, 2001). Therefore, the true polar wander rotations proposed appear to be artifacts related to the fixed hotspot reference frame employed.

Because Late Cretaceous true polar wander predictions are inconsistent with the Pacific observations, we must now consider hotspot motion as an explanation for the difference between the paleomagnetic paleolatitude derived for Detroit Seamount (Tarduno and Cottrell, 1997) and that predicted by a fixed hotspot reference frame. We can isolate the latitudinal history of the Emperor seamounts from that of the Hawaiian chain by subtracting the difference between the present-day latitudes of the 43-Ma bend and Hawaii from the present-day latitudes of each of the Emperor seamounts. In effect, we slide the Emperor trend down the Hawaiian chain to the present-day latitude of Hawaii (Fig. 6). In so doing, we produce a plot predicting the paleolatitude of Emperor seamounts if they were formed by a hotspot moving at constant velocity beneath a stationary plate. The new Detroit Seamount result together with the Suiko Seamount data parallel this predicted trend and provide support for the hotspot motion hypothesis. Differences between the data and predicted values also allow for some northward plate motion. It is difficult to place error bounds on the rate of motion, because there are only two estimates of paleolatitude available. Nevertheless, the data suggest that the Hawaiian hotspot could have moved southward from 81 to 43 Ma (Norton, 1995) at a constant rate of 30-50 mm/yr, while the Pacific plate moved slowly northward in a paleomagnetic (spin axis) frame of reference (Fig. 5).

SCIENTIFIC OBJECTIVES

1. Determining the Paleolatitude and Age of the Emperor Seamount

Interpretations of the Hawaiian-Emperor bend have had a tremendous impact on our understanding of the history and dynamics of plate motions. Diverse new data sets suggest these interpretations may be wrong or at best largely incomplete. Below, we outline a coring plan to test the hypothesis of Hawaiian hotspot motion. Our primary goals are to obtain accurate and precise paleolatitude and

age estimates for each of the five or six sites to be drilled. These data, when compared with fixed and moving hotspot predictions, form the basis of our paleomagnetic test. To accomplish our goals, we have targeted moderate penetration of basalt sections with the aim of obtaining an average of geomagnetic secular variation (≥15 independent paleomagnetic inclination units) at each site. Our sites are divided into three groups having slightly different objectives. Group 1 (Meiji Guyot) is in the northernmost end of the Emperor trend. Here we hope to obtain a new time-averaged paleolatitude and an age constraint for the oldest extant part of the Hawaiian-Emperor chain. Group 2 sites are on Detroit Seamount. Here we hope to improve the precision of prior paleolatitude estimates and possibly obtain new time-averaged paleolatitude data with ages different from those of Detroit Seamount ODP Site 884. Group 3 contains sites on Nintoku, Ojin, and Koko Seamounts. Here we hope to investigate the mechanisms for discrepancies between paleomagnetic data and predictions based on fixed hot-spot models. Combined with data from Suiko Seamount (Kono, 1980), time-averaged paleomagnetic data of known age from these seamounts should allow us to test existing models and potentially develop new models about the role of the mantle in generating the Emperor trend and the Hawaiian-Emperor bend.

The new paleomagnetic data should also allow for the construction of an improved Pacific apparent polar wander path (APWP). In addition to its utility in the study of Pacific plate kinematics, the APWP can provide the basis for improved paleogeographic reconstructions important for paleoclimate studies. Such reconstructions should aid in the use of proxy climate data used to define past latitudinal gradients (e.g., Huber et al., 1995; Zachos et al., 1994), and they may serve as a more stable reference frame than that based on fixed hotspots (Cottrell and Tarduno, 1997b).

Through our drilling approach (obtaining time-averaged paleomagnetic data at each site), we can also address other aspects of the geomagnetic field through Late Cretaceous to early Tertiary time. To fully understand the nature of the geomagnetic field, global data are required. Progress in our understanding of the geomagnetic field over the past 150 m.y. is hindered by the lack of sufficient high-resolution data from the Pacific plate. By targeting sites where a secular variation record can be obtained in basalt, significant advances can be made in our understanding of the time-averaged geomagnetic field and its intensity for Late Cretaceous to early Tertiary times.

2. Investigate The Time-Averaged Late Cretaceous to Early Tertiary Geomagnetic Field

The need for high-resolution paleomagnetic data to constrain this history reaches far beyond the

paleomagnetic community. Recent advances in modeling that have produced realistic simulations of the geodynamo (e.g., Glatzmaier and Roberts, 1995) highlight one need for paleomagnetic constraints on model parameters. The nature and history of the time-averaged geomagnetic field is a major topic of interest for many scientists interested in studies of the Earth's deep interior (SEDI). A full description the past field requires data from the Pacific Ocean basin, because of potential longitudinal components. The geomagnetic field at radius *r*, colatitude θ, and longitude ϕ can be described by the gradient of the harmonic potential Ψ as

$$\Psi(r,\theta,\phi) = a\sum_{l=1}^{\infty}\sum_{m=0}^{l}(a/r)^{l+1}(g_l^m \cos m\phi + h_l^m \sin m\phi)P_l^m(\cos\theta).$$

The Gauss coefficients g_l^m and h_l^m describe the size of spatially varying fields. For the present field and models of the Late Cretaceous to early Tertiary field the axial dipole term (g_1^0) is overwhelmingly dominant. Therefore, other terms will not greatly affect the accuracy of data used to test hotspot motion hypothesis. However, the data obtained can be used to better constrain the Gauss coefficients of the past field. For nonzonal terms ($m \neq 0$; i.e., those terms varying with longitude), data from the Pacific basin are essential because of its sheer size; no global description of the field can be considered complete without data from the region.

Whereas the general importance and need for Pacific data are generally appreciated, the methods used to summarize past data prior to modeling (spherical harmonic analysis) have been given less consideration. For the early Tertiary and Late Cretaceous, plate motion cannot be neglected as they can for analyses of data over the past 5 m.y. (Constable, 1992) but instead the data must be first rotated into a common reference. The few analyses that have tried to incorporate data from the Pacific (principally older seamount results) have relied on a fixed hotspot frame of reference; hence previous estimates of Gauss coefficients may contain considerable errors if the hotspot motion hypothesis is correct.

Interestingly, these analyses show a dramatic change in the Gauss coefficients (a change in sign) during the critical Late Cretaceous to early Tertiary interval we have targeted for study (Livermore et al., 1984) (Fig. 7). Therefore, the data collected at the sites proposed for study can simultaneously

address the hypothesis of hotspot motion and the reality of this change in sign of the spatially varying Late Cretaceous-early Tertiary geomagnetic field.

3. Investigate Late Cretaceous to Early Tertiary Geomagnetic Paleointensity

When compared with the considerable success of studies that utilize directional data derived from paleomagnetic measurements, work devoted to understanding the past intensity of the geomagnetic field has advanced more slowly. However, the long-term variations of paleointensity are essential for a complete description of the field, as well as for understanding the long-term magnetic signature of ocean crust. One reason progress has been slow is related to selection criteria needed to ensure reliable paleointensity determination. The preferred method of paleointensities measurement, Thellier-Thellier double heating experiments of basalts (Thellier and Thellier, 1959; as modified by Coe, 1967), often encounter problems due to chemical alteration during heating. Significant recent progress has been made by studying basaltic glass (Pick and Tauxe, 1993), which shows ideal magnetic properties. The available DSDP and ODP sites having basaltic glass have now been analyzed (Juarez et al., 1998), so further progress requires additional drilling (Fig. 7).

The coring we propose has the potential to yield several reference sites for Late Cretaceous-early Tertiary paleointensity. Because we propose to sample a significant number of flow units at each site cored, the chances of obtaining a time-averaged paleointensity value at our site are greatly increased. Even if basaltic glass is not recovered, recent advances in paleointensity measurements measured on single plagioclase crystals (Cottrell and Tarduno, 1997a; Cottrell and Tarudno, 1999) may allow considerable new paleointensity data to be recovered for the Late Cretaceous to early Tertiary interval. Magnetic inclusions contained within such feldspars have been shown to yield paleointensity data less affected by experimental alteration (Cottrell and Tarduno, 2000). We hope to explore whether time-averaged estimates of paleointensity (Tarduno et al., 2001) can be obtained through the investigation of multiple lava flows at each site.

4. Source and Melting History of the Hawaiian Hotspot

Hotspots are of continuing interest to mantle geochemists because they provide "windows" into parts of the mantle that lie beneath the upper mantle source region for midocean ridges. An observed range of distinct mantle compositions offers the means to investigate such important issues as the geochemical evolution of the mantle, temporal and spatial scales of mantle convection, and lithosphere-mantle interactions. No hotspot has been more intensely examined from a

geochemical perspective than Hawaii through compositional studies of lava sequences from the islands at the southeast end (e.g., Chen and Frey, 1985; Garcia et al., 1998) to dredged and drilled rocks from about 30 sites along this prominent and long-lived lineament (e.g., Lanphere et al., 1980; Clague and Dalrymple, 1987; Lonsdale et al., 1993; Keller et al., 2000).

As an example, the Sr-isotope ratios of tholeiitic basalts from the Hawaiian hotspot track show a systematic trend through time (Fig. 8). These ratios are approximately constant along the Hawaiian Ridge (out to the 43-Ma bend) then decrease steadily northwards along the Emperor seamounts to Suiko. This decrease has been attributed to a decrease in distance between the hotspot and the nearest spreading ridge (Lanphere et al., 1980). Only the tholeiitic basalts from the shield phase of volcano construction show this trend, because only these magmas appear to have escaped contamination with the oceanic lithosphere (Chen and Frey, 1985). Keller et al. (2000) have extended this analysis to Detroit and Meiji Seamounts, and find that Sr-isotope ratios continue to decrease northward, with a minimum value at Detroit well within the range of compositions for Pacific midocean ridge basalts (MORB). This composition (confirmed with other isotopic and elemental ratios) is unprecedented in the Hawaiian hotspot-produced volcanism to the south but is consistent with the interpretation from plate reconstructions that the hotspot was located close to a spreading ridge at ~80 Ma. The seamount magmas, then, appear to be derived from a mixture of plume- ("enriched") and predominantly asthenosphere ("depleted") mantle sources. The plume end-member is more like the "Kilauea" than the "Koolau" component of the modern hotspot.

A consideration of the age of seafloor surrounding the northern Emperor Seamounts (e.g., Mammerickx and Sharman, 1988) suggests a spreading ridge was (e.g., Mammerickx and Sharman, 1988) close to the Hawaiian hotspot at ~80 Ma. In other locations where a plume is close to a ridge (e.g., Galapagos, Easter, and Iceland), the isotopic compositions of hotspot products extend toward MORB values. Several processes may lead to this effect: the nearby spreading ridge could have provided a higher temperature and lower viscosity/density regime leading to significant entrainment of aesthenosphere within the rising plume. Thinner lithosphere near the ridge would promote a longer melting column in the plume leading to greater entrainment and homogenization of geochemical heterogeneities. Also, younger hotter lithosphere may be more readily assimilated by the ascending plume melts. Thus, the thickness of the lithosphere could determine how much asthenosphere contributes to hotspot volcanism. Finally, a change in the isotopic characteristics of the plume itself through time cannot be ruled out. The (deep mantle?) region where the Hawaiian

plume acquires its geochemical characteristics has probably not been homogeneous and static. But the degree of geochemical variability at given sites within the Emperor seamounts has not been established on the basis of the few analyses reported so far.

Geochemical data for lava flows from the Emperor seamounts sites will be produced to document the compositional and thermal characteristics of mantle sources and melting conditions of the early history of the Hawaiian hotspot. Major and trace element abundances will place limits on the depth and extent of melting and track magma evolution (fractionation, contamination) to the surface. Such data will also categorize magmas as tholeiitic, alkalic, or post-erosional for comparison with Hawaiian islands construction. Isotopic work (Sr, Nd, Pb, and Hf isotope ratios, parent-daughter measurements of whole rocks, and He for glasses and fresh olivine if these are recovered) will identify mantle-source components. Other studies, such as volatiles in glasses, are planned depending on suitable material.

Knowledge of the physical volcanology of the lava flows at Emperor seamount sites is important for understanding the mechanisms and time scales of eruptions. Studies of the physical characteristics of historic lava flows at Hawaii have led to the means of linking outcrop-scale observations to important eruption parameters, such as flow volume, velocity, viscosity, and distance from source. From the recovered core and logging records, we will measure flow thickness, direction, structure, vesicularity, crystallinity, and estimate the duration of intervals between flows. This information will be integrated with evidence for eruptive environment (submarine vs. subaerial, volcano flank vs. summit) and secular variation measurements from the paleomagnetic studies to estimate timescales for the recovered sections.

DRILLING STRATEGY

Secular Variation in Previous Ocean Drilling Studies

A key question concerning paleomagnetic tests such as those proposed here is the penetration needed to average adequately secular variation. It has been suggested that recent drilling on Hawaii should be taken as a guide. In our view, the best estimate of the depth of penetration needed is provided by previous drilling in the Emperor chain. This drilling record provides a better temporal gauge of the waning stages of basalt extrusion on seamounts 50-90 Ma. Drilling on Detroit

Seamount indicates that as little as 85 m of basalt penetration may be needed at some sites to obtain an average of secular variation. When basalt penetration was greater than 120 m during previous coring of Cretaceous plateaus, seamounts, and guyots in the Pacific, enough independent time units were recovered to average secular variation (Tarduno and Sager, 1995; Tarduno and Gee, 1995). This value does not differ greatly from the depth range over which secular variation is averaged (100-200 m) in analyses of basalt cores obtained by drilling on Hawaii (Holt et al., 1996). However, it is not possible to determine prior to drilling the time sequence represented by the lava flows at a given site. We must evaluate the angular dispersion of independent flow (inclination) units and compare this value with global paleomagnetic data to confirm whether secular variation has been adequately sampled at a given site. It is possible to collect paleomagnetic data at sea and to make these calculations during coring to insure the resulting record will provide an adequate average.

Paleolatitude Experiment

We propose to drill five to six basement sites along the Emperor seamounts chain. We group the drilling sites and order as follows: Group 1 will be at the oldest (northern) end of the chain, Group 2 at Detroit Seamount, and Group 3 at seamounts south of Detroit, along the youngest portion of the chain. All sites will be drilled and cored using the rotary core barrel (RCB). We propose basement penetrations to moderate depth (150-250 m). At the northern sites with thicker sediment cover, our strategy will be to employ minicones for reentry after a single bit change.

Site survey data used in the approval of these DSDP/ODP locations have been used to guide our proposed coring. For each site proposed, previous nearby DSDP or ODP coring has touched basement or penetrated the sediment cover, providing information on the nature of the sediments and basement depth as well as drilling times. We propose to drill without coring through the sediments to a few cores above the basement because (1) these sediments have been cored previously, (2) there is problem with bias in paleomagnetic inclinations derived from sediments, and (3) time saved can be used toward coring more of the lava flow sequences. An exception to this plan is the Meiji Seamount site (see below). We have estimated depths for the basement penetration based on drilling of other Pacific seamount and plateau sites (e.g., Legs 143, 144, and 192). Whereas these estimates are needed for the planning process, we envision an interactive process based on the recovery. We hope to recover at least 15 flow units at each site for detailed paleomagnetic and radiometric age ($^{40}Ar/^{39}Ar$) analysis. If this is achieved in a given hole, we

would prefer to drill additional sites on a seamount (or additional seamounts) to improve the accuracy of paleolatitude determinations and assist in the overall test. Below we include a brief description and rationale for each of the drilling sites.

Group 1: Meiji Seamount (~86 Ma)

A precisely determined paleolatitude from a well-dated site in the northernmost Emperor Seamount is of the highest priority. Given the new age data from Leg 145, the age of Meiji Seamount is presumably older than 81 Ma but how much older is uncertain. There is also a bend in the northern Emperor trend that, if better dated, could be used to examine independently some of the issues of plate and hotspot motion discussed here. We identified two sites on Meiji Seamount (Figs. 1, 9) near DSDP Site 192. If the current trend of the Emperor paleomagnetic data reflects continuous hotspot motion, we expect to find a paleolatitude of ~40° for Meiji. Site HE-1A, at the location of DSDP Site 192, is our alternate site on Meiji Guyot. Prior drilling at DSDP Site 192 indicates a sediment cover of 1044 m, composed of ooze, chalk, and clays above subaerial basalt. Our primary site (HE-1B) is located 6 km southwest of DSDP Site 192. We expect this site to have a thinner sediment cover than that penetrated at Site 192. However, the sediment cover should include a relatively thick (200-300 m?) section of Paleogene to Cretaceous sediments of paleoceanographic importance that we plan to core before penetrating basement. We note that failure to obtain clearance for drilling on Meiji Guyot (which is in Russian territorial waters) will force us to adopt an alternate drilling strategy. If clearance is denied, we will drill two primary sites on Detroit Seamount (see below) or, should a seismic data package be prepared (and approved by the appropriate JOIDES panels) prior to the leg, a site on the ridge between Meiji Guyot and Detroit Seamount in international waters.

Group 2: Detroit Seamount (81 Ma)

We identified five potential drill sites on Detroit Seamount. With paleolatitude data from one or more of these sites, we expect to improve the existing time-averaged results available from just a single site (Site 884) (Tarduno and Cottrell, 1997). Primary Site HE-3B is located on the summit region of Detroit Seamount between ODP Sites 882 and 883 and has a relatively thin (<500 m) sediment cover. Site HE-3A (an alternate site if clearance is obtained for drilling on Meiji Guyot or a primary site if clearance is denied) is in a similar region and has a similar sedimentary thickness above basement. Alternate Site HE-2 is located 7 km northwest of ODP Site 882 and has a

sediment column composed of ~800 m of oozes, chalks, and clays. Alternate Site HE-3 is ODP Site 883, where the sediment column above basaltic basement is 840 m thick.

Group 3: Nintoku (≥56 Ma), Ojin (56 Ma), and Koko Seamounts (≥48 Ma)

Present paleomagnetic data from basalt cores are insufficient to determine how the 8° paleolatitude discrepancy between Suiko Seamount and present-day Hawaii accumulated and the potential relative contributions of true polar wander and hotspot motion in causing the discrepancy. We propose drilling Nintoku and Ojin Seamounts and Koko Guyot (Figs. 1-9) to examine this question. Paleolatitude results can also be compared with global data to test for true polar wander. We note that at these sites the difference in measured paleolatititude with present Hawaii may be quite small, so the number of independent cooling units (flows) needed for a significant statistical test will be larger and require penetration greater than that at the more northerly sites (or additional sites on each seamount or guyot). We are helped somewhat in that the decreased angular dispersion of paleomagnetic directions at the lower latitudes of these sites, however, acts to allow a more precise paleolatitude estimate for a given number of independent flow units.

If the Emperor trend represents southward hotspot motion of the Hawaiian hotspot, we should obtain a paleolatitude of 25°-27° for Nintoku Seamount. Two sites have been identified on Nintoku Seamount. Proposed alternate Site HE-4A is positioned at DSDP Site 432A, near the northwest edge of the seamount on flat-lying stratified sediments. Previous drilling indicates the sediments are 42 m thick above the lava flows. The uppermost flows are separated by soil horizons, indicating significant time between cooling units. Primary Site HE-4B is offset by ~28 km to the northwest on the volcano summit. Geochemical and radiometric age data from Nintoku Seamount, however, indicate that prior drilling at DSDP Site 432 penetrated late-stage alkalic lavas (Dalrymple et al., 1980). Although such alkalic rocks are suitable for paleomagnetic tests, it is desirable to obtain as wide an age range as available. Accordingly, we will use short seismic surveys during the leg to evaluate whether a suitable flank site free of tectonic complications can be identified (i.e., whether early tholeiitic shield lavas might be sampled).

Four sites have been identified on Ojin Seamount. Alternate Site HE-5A is positioned on Ojin Seamount at DSDP Site 430 (Figs. 1, 9). Approximately 60 m of sediments (ooze, sand, and volcanic ash) overlie lava flows at this site. Alternate Site HE-5B is located to the northeast of

DSDP Site 430 on the summit flank. Sites HE-5C and HE-5D are on the seamount summit to the east of DSDP Site 430. Site HE-5C is designated as the primary site.

Primary Site HE-6A is positioned at DSDP Site 308 (Figs. 1, 9) on Koko Guyot. Previous drilling penetrated ~70 m of clays and volcaniclastic sandstone. Our alternate Site HE-6B is located at DSDP Site 309. Although previous DSDP drilling at those sites was also terminated prior to penetrating basement, they are located in sedimented areas where drilling can be easily started.

UNDERWAY GEOPHYSICS

Standard ODP practice is to collect magnetometer and 3.5- and 12-kHz echo sounder data during transit to each site. Additionally, we will conduct short single-channel seismic reflection surveys using twin 80-in^3 Seismic Systems Inc. (SSI) water guns with single lines over sites at Nintoku Seamount, Ojin Seamount, and Koko Guyot and crossing lines over the northernmost sites.

SAMPLING STRATEGY

The Sample Distribution, Data Distribution, and Publications Policy is posted at: http://www-odp.tamu.edu/publications/policy.html. As part of this policy, any sampling to be conducted during Leg 197 or during the one year moratorium following the end of the leg must be approved by the Sampling Allocation Committee (SAC), consisting of the co-chiefs, staff scientist, and curatorial representative.

Sample requests may be submitted by shore-based and shipboard scientists, preferably three months before the beginning of the cruise via the electronic form (http://www-odp.tamu.edu/curation/subsfrm.htm). About two months precruise, the SAC will prepare a temporary sampling plan, which will be revised on the ship as needed. Minimizing redundancy of measurements among the science party, both shipboard and shore-based scientists, will be a factor in evaluating sample requests. The sampling plan will be subject to modification depending upon the actual material recovered and collaborations that may evolve between scientists during the leg.

Shipboard and Shore-Based Samples

We wish to emphasize that given our paleomagnetic objectives, maintaining the orientation of core pieces is critical for the success of the leg. Therefore, special labeling and sampling procedures may be developed to ensure that core handling and sampling does not compromise core piece orientations. We plan to RCB core a single hole at each site and to drill rather than core part of the sedimentary section at the Meiji Guyot and Detroit Seamount sites as indicated in Table 1. Samples for shipboard studies will be collected following core labeling, nondestructive whole-core measurements (multi-sensor track measurements and core images taken for core reorientation), core splitting, and further labeling of individual pieces of core (including orientation labeling). The shipboard samples will be collected from working halves of cores by the shipboard party.

Given the paleomagnetic objectives for the leg, we anticipate collecting a large number of oriented samples for reconnaissance shipboard paleomagnetic measurements. The paleomagnetic data from these shipboard samples will be used to assess on site whether secular variation has been averaged by the recovered lava flows. However, shipboard samples should not be taken in a way that compromises (or destroys) the orientation of the core piece. Other shipboard samples will also be collected at this time for shipboard geochemical and mineralogical analyses, for making polished thin sections, and for physical properties measurements. Similarly, these samples must be taken in a way that does not compromise the unambiguous orientation of core pieces.

Samples for shore-based studies will be collected toward the end of the cruise to devise sampling strategies that take advantage of the information obtained from the shipboard measurements. Generally, shipboard scientists may obtain up to 100 samples in volcanic units, with the size of individual samples being <15 cm^3 in most cases. In special cases, additional or larger samples may be obtained with the approval of the SAC. Soon after the cores return to the ODP Gulf Coast repository, additional samples may be obtained upon written request.

Short intervals of unusual scientific interest (e.g., K/T boundary sections, veins, ores, glass, and dikes) may require careful handling, higher sampling density, reduced sample size, continuous core sampling by a single investigator, or use of sampling techniques not available on board the ship. These intervals will be identified during the core description process, and a specific sampling protocol will be established by the interested scientists and the shipboard SAC.

LOGGING PLAN

Downhole logging will be used during Leg 197 to address issues concerning possible deviation of holes from vertical, in situ basalt magnetizations, core orientation, volcanic stratigraphy, and eruptive morphology. Whereas core recovery is often biased and incomplete in lithologies such as alternating pillows and massive flows, logging data are continuous and therefore provide useful information over intervals of low core recovery. During Leg 197, we are particularly interested in determining the number of flow units, which has implications for how well geomagnetic secular variation has been sampled, and hence, how well paleomagnetic paleolatitudes can be constrained. If time permits, we also plan to use logging data to create synthetic seismograms, which will then lead to improved correlation between the seismic records and the lithologic units recovered from the boreholes. As shown in the Operations Schedule (Table 1), we tentatively plan to log at each site. Subject to time constraints, this logging plan may be adjusted at the discretion of the co-chiefs within the guidelines of the normal JOIDES logging policy.

To achieve the Leg 197 scientific objectives, the proposed sites will be logged with the standard logging tool strings (triple combination [triple combo] and Formation MicroScanner [FMS]). Specifically the logging plan includes one triple combo and one FMS run along the whole drilled section and a second FMS run in the basalt intervals. A triple combo run and one FMS run may be extended into the sedimentary section depending on time constraints. The characteristics of these logging tool strings can be found at the Borehole Research Group web site at http://www.ldeo.columbia.edu/BRG and are briefly described in the next paragraph.

- The triple combo tool string consists of several probes recording geophysical measurements of the penetrated formations. It consists of the accelerator porosity sonde (APS), which gives the porosity from epithermal neutron measurements, and the hostile environment lithodensity sonde (HLDS), which measures bulk density and photoelectric absorption through the interaction of gamma rays with electrons in the formation.The hostile environment natural gamma ray sonde (HNGS) and natural gamma ray tool are used to measure the natural radioactivity of the drilled formation.The resistivity tool should aid in identification of lava flows in the upper oceanic crust. The resistivity of the basaltic rocks is rather high and will likely exceed 2000 Ohm-m, so the dual laterolog (DLL) will be used in combination with the triple combo to ensure that reliable resistivity data are collected.

- The FMS provides high-resolution electrical images of the penetrated formations. We will attempt to azimuthally reorient the cores by identifying fractures and veins in the FMS images that can be correlated with their counterparts on the recovered core. The FMS tool string also includes the general purpose inclinometry cartridge (GPIT), which provides accelerometer and magnetometer data to allow determination of the tool position and spatial orientation of the images. The GPIT will also be used to constrain the deviation of the hole from vertical, which is an important factor in evaluating possible biases in paleolatitude estimates derived from paleomagnetic measurements on the core.

  If time allows, the dipole sonic imager (DSI) will be used to measure the compressional and shear wave velocities. The natural gamma ray tool (NGT) is run in combination with the previous probe to achieve depth matching between the different logging runs. Importantly, the DSI will be run separately from the FMS/GPIT because it will otherwise introduce a large spurious magnetic signal in the GPIT data. The GPIT data and their use in the calculating hole deviation are of highest priority in terms of leg objectives.

In addition, we plan to log one site with a magnetic logging tool being developed by the Geophysical Institute of the University of Göttingen, Federal Republic of Germany (referred to as the Göttingen Borehole Magnetometer [GBM]), and with a third-party magnetic susceptibility borehole tool (referred to as the SUSLOG 403-D). The GBM has three fluxgate sensors that measure three orthogonal components of the magnetic field, whereas the SUSLOG 403-D obtains an estimate of bulk magnetic susceptibility useful for modeling the contributions of induced magnetizations to the total magnetic signal recorded by the GBM. The effectiveness of these tools will be evaluated during the leg, and, time allowing, they may be run at additional sites.

REFERENCES

Acton, G.D., and Gordon, R.G., 1994. Paleomagnetic tests of Pacific plate reconstructions and implications for motions between hotspots. *Science* 263:1246-1254.

Arason, P., and Levi, S., 1990. Compaction and inclination shallowing in deep-sea sediments from the Pacific Ocean. *J. Geophys. Res.,* 95:4501-4510.

Atwater, T., 1989. Plate tectonic history of the northeast Pacific and western North America. *In* Winterer, E.L., Hussong, D.M., and Decker, R.W. (Eds.), *The Eastern Pacific Ocean and Hawaii,* Geol. of North America Ser., N:21-72.

Besse, J., and Courtillot, V., 1991. Revised and synthetic apparent polar wander paths of African, Eurasian, North American and Indian plates, and true polar wander since 200 Ma. *J. Geophys. Res.,* 96:4029-4051.

Butler, R.F., 1992. *Paleomagnetism, Magnetic Domains to Geologic Terranes*: Boston (Blackwell).

Cande, S.C., Raymond, C.A., Stock, J., and Haxby, W.F., 1995. Geophysics of the Pitman Fracture Zone and Pacific-Antarctic plate motions during the Cenozoic. *Science*, 270:947-953.

Celaya, M.A., and Clement, B.M., 1988. Inclination shallowing in deep sea sediments from the North Atlantic. *Geophys. Res. Lett*., 15:52-55.

Chen, C.-Y., and Frey, F.A., 1985. Trace element and isotopic geochemistry of lavas from Haleakala volcano, East Maui, Hawaii: implications for the origin of Hawaiian basalts. *J. Geophys. Res.,* 90:8743-8768.

Christensen, U., 1998. Fixed hotspots gone with the wind. *Nature*, 391:739-740.

Clague, D.A., and Dalrymple, G.B., 1987. The Hawaiian-Emperor volcanic chain, Part I, Geologic evolution. *Geol. Surv. Prof. Pap. U.S.,* 1350:5-54.

Coe, R.S., 1967. Paleo-intensities of the Earth's magnetic field determined from Tertiary and Quaternary rocks. *J. Geophys. Res*., 72:3247-3262.

Constable, C., 1992. Link between geomagnetic reversal paths and secular variation of the field over the past 5 Myr. *Nature*, 358:230-233.

Cottrell, R., and Tarduno, J.A., 1997a. Magnetic hysteresis properties of single crystals: prelude to paleointensity studies, *Eos*, 78:F185.

Cottrell, R.D., and Tarduno, J.A., 1997b. Tectonic and paleoclimatic implications of a high latitude Late Cretaceous pole position for the Pacific plate. *Eos,* 78:S117.

Cottrell, R.D., and Tarduno, J.A., 2000a. In search of high fidelity geomagnetic paleointensities: a comparison of single plagioclase crystal and whole rock Thellier-Thellier analyses. *J. Geophys. Res.,* 105:23579-23594.

Cottrell, R.D., and Tarduno, J.A., 2000b. Late Cretaceous true polar wander: not so fast. *Science*, 288:2283a.

Cox, A.V., 1970. Latitude dependence of the angular dispersion of the geomagnetic field. *Geophys. J. R. Astron. Soc*., 20:253-269.

Dalrymple, G.B., Lanphere, M.A., and Clague, D.A., 1980. Conventional and $^{40}Ar/^{39}Ar$ K-Ar ages of volcanic rocks from Ojin (Site 430), Nintoku (Site 432) and Suiko (Site 433) seamounts and the chronology of volcanic propagation along the Hawaiian-Emperor Chain. *In* Jackson, E.D., Koizumi, I., et al., *Init. Repts. DSDP,* 55: Washington (U.S. Govt. Printing Office), 659-676.

deMenocal, P.B., Ruddiman, W.F., and Kent, D.V., 1990. Depth of post-depositional remanence acquisition in deep-sea sediments: a case study of the Brunhes-Matuyama reversal and oxygen isotopic Stage 19.1. *Earth. Planet. Sci. Lett*., 99:1-13.

D'Hondt, S., and Arthur, M.A., 1996. Late Cretaceous oceans and the cool tropic paradox. *Science*, 271:1838-1841.

Duncan, R.A., and Clague, D.A., 1985. Pacific plate motion recorded by linear volcanic chains. *In* Nairn, A.E.M., Stehli, F.G., Uyeda, S. (Eds.), *The Ocean Basins and Margins*, (Vol. 7A): New York (Plenum), 89-121.

Duncan, R.A., and Richards, M.A., 1991. Hotspots, mantle plumes, flood basalts, and true polar wander. *Rev. Geophys*., 29:31-50.

Garcia, M.O., Ito, E., Eiler, J.M., and Pietruszka, A.J., 1998. Crustal contamination of Kilauea volcano magmas revealed by oxygen isotope analyses of glass and olivine from Puu Oo eruption lavas. *J. Petrol*., 39:803-817.

Gee, J., Staudigel, H., and Tauxe, L., 1989. Contribution of induced magnetization to magnetization of seamounts. *Nature,* 342:170-173.

Glatzmaier, G.A., and Roberts, P.H., 1995. A 3-dimensional self-consistent computer-simulation of a geomagnetic-field reversal. *Nature*, 377:203-209.

Goldreich, P., and Toomre, A., 1969. Some remarks on polar wandering. *J. Geophys. Res*., 74:2555-2567.

Gordon, R.G., 1983. Late Cretaceous apparent polar wander of the Pacific plate: evidence for a rapid shift of the Pacific hotspots with respect to the spin axis. *Geophys. Res. Lett.*, 10:709-712.

Gordon, R.G., 1990. Test for bias in paleomagnetically determined paleolatitudes from Pacific Plate Deep Sea Drilling Project sediments, *J. Geophys. Res.*, 95:8397-8404.

Gordon, R.G., and Cape, C., 1981. Cenozoic latitudinal shift of the Hawaiian hotspot and its implications for true polar wander. *Earth Planet. Sci. Lett.*, 55:37-47.

Hodych, J.P., and Bijaksana, S., 1993. Can remanence anisotropy detect paleomagnetic inclination shallowing due to compaction? A case study using Cretaceous deep-sea limestones. *J. Geophys. Res.*, 98:22429-22441.

Holt, J.W., Kirschvink, J.L., and Garnier, F., 1996. Geomagnetic field inclinations for the past 400 kyr from the 1-km core of the Hawaii Scientific Drilling Project. *J. Geophys. Res.*, 101:11655-11663.

Huber, B.T., Hodell, D.A., and Hamilton, C.P., 1995. Mid- to Late Cretaceous climate of the southern high latitudes: stable isotopic evidence for minimal equator-to-pole thermal gradients. *Geol. Soc. Am. Bull.*, 107:1164-1191.

Jackson, M.J., Banerjee, S.K., Marvin, J.A., Lu, R., and Gruber, W., 1991. Detrital remanence, inclination errors, and anhysteretic remanence anisotropy: quantitative model and experimental results. *Geophys. J. Int.*, 104:95-103.

Juarez, M.T., Tauxe, L., Gee, J.S., and Pick, T., 1998. The intensity of the Earth's magnetic field over the past 160 million years. *Nature*, 394:878-881.

Keller, R.A., Duncan, R.A., and Fisk, M.R., 1995. Geochemistry and $^{40}Ar/^{39}Ar$ geochronology of basalts from ODP Leg 145 (North pacific Transect). *In* Rea, D.K., Basov, I.A., Scholl, D.W., and Allan, J.F. (Eds.), *Proc. ODP, Sci. Results*, 145: College Station, TX (Ocean Drilling Program), 333-344.

Keller, R.A., Fisk, M.R., and White, W.M., 2000. Isotopic evidence for Late Cretaceous plume-ridge interaction at the Hawaiian hotspot. *Nature*, 405:673-676.

King, R.F., 1955. Remanent magnetism of artificially deposited sediments. *Mon. Not. R. Astron. Soc. Geophys. Suppl.*, 7:115-134.

Kodama, K.P., and Sun, W.W., 1992. Magnetic anisotropy as a correction for compaction-caused paleomagnetic inclination shallowing. *Geophys. J. Int.,* 111:465-469.

Kono, M., 1980. Paleomagnetism of DSDP Leg 55 basalts and implications for the tectonics of the Pacific plate. *In* Jackson, E.D., Koizumi, I., et al., *Init. Repts. DSDP*, 55: Washington (U.S. Govt. Printing Office), 737-752.

Lanphere, M.A., Dalrymple, G.B., and Clague, D.A., 1980. Rb-Sr systematics of basalts from the Hawaii-Emperor volcanic chain. *In* Jackson, E.D., Koizumi, I., et al., *Init. Repts. DSDP*, Washington (U.S. Govt. Printing Office), 55:695-706.

Larson, R.L., Steiner, M.B., Erba, E., and Lancelot, Y., 1992. Paleolatitudes and tectonic reconstructions of the oldest portion of the Pacific Plate: a comparative study. *In* Larson, R.L., Lancelot, Y., et al., *Proc. ODP, Sci. Result*s, 129: College Station, TX (Ocean Drilling Program), 615-631.

Livermore, R.A., Vine, F.J., and Smith, A.G., 1984. Plate motions and the geomagnetic field II. Jurassic to Tertiary. *Geophys. J. R. Astron. Soc.,* 79:939-961.

Lonsdale, P., Dieu, J., and Natland, J., 1993. Posterosional volcanism in the Cretaceous part of the Hawaiian hotspot trail. *J. Geophys. Res.*, 98:4081-4098.

McFadden, P.L., Merrill, R.T., McElhinny, M.W., and Lee, S., 1991. Reversals of the Earth's magnetic field and temporal variations of the dynamo families. *J. Geophys. Res.*, 96:3923-3933.

McFadden, P.L., and Reid, A.B., 1982. Analysis of paleomagnetic inclination data. *Geophys. J. R. Astron. Soc*., 69:307-319.

Mammerickx, J., and Sharman, G.F., 1988. Tectonic evolution of the North Pacific during the Cretaceous quiet period. *J. Geophys. Res*., 93:3009-3024.

Molnar, P., and Atwater, T., 1973. Relative motion of hotspots in the mantle. *Nature* 246:288-291.

Molnar, P., and Stock, J., 1987. Relative motions of hotspots in the Pacific, Atlantic and Indian Oceans since late Cretaceous time. *Nature*, 327:587-591.

Morgan, W.J., 1971. Convection plumes in the lower mantle. *Nature*, 230:42-43.

Norton, I.O., 1995. Plate motions in the North Pacific: the 43 Ma Nonevent. *Tectonics*, 14:1080-1094.

Parker, R.L., 1991. A theory of ideal bodies for seamount magnetization. *J. Geophys. Res*., 96:16101-16112.

Pick, T., and Tauxe, L., 1993. Geomagnetic paleointensities during the Cretaceous normal superchron measured using submarine basaltic glass. *Nature*, 366:238-242.

Rea, D.K., Basov, I.A., Scholl, D.W., and Allan, J.F. (Eds.), 1995. *Proc. ODP, Sci. Results*, 145: College Station, TX (Ocean Drilling Program).

Sager, W.W., and Bleil, U., 1987. Latitudinal shift of Pacific hotspots during the Late Cretaceous and early Tertiary. *Nature*, 326:488-490.

Sager, W.W., and Pringle, M.S., 1988. Mid-Cretaceous to Early Tertiary apparent polar wander path of the Pacific Plate. *J. Geophys. Res.*, 93:11753-11771.

Solomon, S.C., Sleep, N.H., and Jurdy, D.M., 1977. Mechanical models for absolute plate motions in the Early Tertiary. *J. Geophys. Res.*, 82:203-213.

Steinberger, B., 1996. Motion of hotspots and changes of the Earth's rotation axis caused by a convecting mantle. [M.S. thesis]. Harvard Univ.

Steinberger, B., 2000. Plumes in a convecting mantle: models and observations for individual hotspots. *J. Geophys. Res.,* 105:11127-11152.

Steinberger, B., and O'Connell, R.J., 1997. Changes of the Earth's rotation axis owing to advection of mantle density heterogeneities. *Nature*, 387:169-173.

Steinberger, B., and O'Connell, R.J., 1998. Advection of plumes in mantle flow: implications for hotspot motion, mantle viscosity and plume distribution. *Geophys. J. Int.*, 132:412-434.

Sun, W.W., and Kodama, K.P., 1992. Magnetic anisotropy, scanning electron microscopy and X-ray pole gonionmetry study of inclination shallowing in a compacting clay-rich sediment. *J. Geophys. Res.*, 97:19599-19615.

Tarduno, J.A., 1990. Absolute inclination values from deep sea sediments: a reexamination of the Cretaceous Pacific record. *Geophys. Res. Lett.,* 17:101-104.

Tarduno, J.A., and Cottrell, R., 1997. Paleomagnetic evidence for motion of the Hawaiian hotspot during formation of the Emperor Seamounts. *Earth Planet. Sci. Lett.*, 153:171-180

Tarduno, J.A., Cottrell, R.D., and Smirnov, A.V., 2001. High geomagnetic field intensity during the mid-Cretaceous from Thellier analyses of single plagioclase crystals. *Science,* 291:1179-1183.

Tarduno, J.A., and Gee, J., 1995. Large scale motion between Pacific and Atlantic hotspots. *Nature*, 378:477-480.

Tarduno, J.A., and Sager, W.W., 1995. Polar standstill of the mid-Cretaceous Pacific plate and its geodynamic implications. *Science,* 269:956-959.

Tarduno, J.A., and Smirnov, A.V., 2001. Stability of the Earth with respect to the spin axis for the last 130 million years. *Earth Planet. Sci. Lett.,* 184:549-553.

Thellier, E., and Thellier, O., 1959. Sur l'intensite du champ magnétique terrestre dans le passé historique et geologique. *Ann. Geophys.,* 15:285-375.

Vasas, S.M., Gordon, R.G., Petronotis, K.E., 1994. New paleomagnetic poles for the Pacific plate from analysis of the shapes of anomalies 33N and 33R. *Eos*, 75:203.

Verosub, K.L., 1977. Depositional and postdepositional processes in the magnetization of sediments. *Rev. Geophys. Space Phys.*, 15:129-143.

Wessel, P., and Kroenke, L.W., 1998. Factors influencing the locations of hotspots determined by the hot-spotting technique. *Geophys. Res. Lett.*, 25:555-558.

Zachos, J.C., Stott, L.D., and Lohmann, K.C., 1994. Evolution of early Cenozoic marine temperatures. *Paleoceanography*, 9:353-387.

FIGURE CAPTIONS

Figure 1. Location of proposed drill areas (open boxes) and previous DSDP and ODP sites (solid dots).

Figure 2. **A.** Preferred viscosity structure used to calculate hotspot motion from Steinberger and O'Connell (1998). A low-viscosity upper mantle is used to reproduce the Hawaiian-Emperor bend. A high-viscosity lower mantle is employed; otherwise the relative motions between hotspots are greater than observations. The Harvard tomographic model S12WM13 was used to infer mantle density heterogeneities. The gradual increase in viscosity was chosen to minimize disagreements with models based on postglacial rebound, which mainly constrain viscosity in the upper half of the mantle. **B.** The predicted motion of the Hawaiian plume between 90 and 43 Ma after Steinberger (2000). The model predicts a southward component of motion ~10 mm/yr. This results from the mantle flow at depth, which also tends to have a southward component of the same magnitude partly due to a return flow opposite to Pacific plate motion assumed in the model. The model predicts only a small relative motion between the Hawaiian and Louisville hotspots, in accordance with the age progressions observed along the two hotspot tracks. Other models with a lower viscosity in the lower mantle predict substantially higher flow speeds and substantially larger southward motion of the Hawaiian hotspot.

Figure 3. Evidence for compaction-induced inclination error in Pacific deep-sea sediments from Tarduno (1990). **A.** DSDP sites with sediment-based paleomagnetic data obtained using thorough demagnetization techniques. **B.** Test for bias in sediment-based paleomagnetic inclinations using 27 age groups. I_o is the observed inclination. I_e is the expected inclination derived from nonsediment sources. A least-squares fit yields a slope, f = 0.52. A delete-1 jackknife resampling shows that the data reject the hypothesis of zero flattening (f = 1) at the 95% confidence interval. **C.** Inclination error vs. expected inclination for f = 0.5 (circles). Open squares = the maximum error in inclination caused by a 5° error in the reference pole, where p is the colatitude. Filled squares = the combined effect of inclination shallowing caused by compaction and an error in the reference pole.

Figure 4. Inclination errors caused by sediment compaction plotted vs. expected inclination values. Curves show the relationship.

$$\tan I_o = f \tan I_e,$$

where I_o = the observed (measured) paleomagnetic inclination, I_e = the expected inclination and f = a variable describing the degree of compaction-induced inclination shallowing. A value of f = 0.52 was derived from paleomagnetic analyses of deep-sea sediments from the Pacific plate (Tarduno, 1990). **A.** The gray box shows the range of inclination values expected for the fixed-hotspot vs. moving-hotspot hypotheses. The expected inclination value for a fixed hotspot is derived from Hawaii's current position, whereas values for Nintoku, Detroit, and Meiji are based on the hypothesis that their location along the Emperor trend records mainly motion of the Hawaiian hotspot. Because the hotspot-motion hypothesis predicts these Emperor seamounts formed at mid-latitudes, errors in sedimentary inclinations induced by compaction will be near their maximum potential values, assuming flattening factors similar to those derived from Cretaceous deep sea sediments from the Pacific. **B.** The expected difference in inclination between the fixed-hotspot and moving-hotspot models (gray box and horizontal dashed lines) shown against compaction-induced inclination error curves. Given a flattening factor of 0.52, the potential error in sediment-based inclination is larger than the signal of hotspot motion proposed for testing for Detroit and Meiji seamounts, the error is two-thirds of the signal proposed for testing.

Figure 5. **A.** Average inclination values for three inclination-group models from Detroit Seamount. Errors are 95% confidence interval. Also shown is the predicted inclination at 81 Ma based on prior Pacific apparent polar wander path (APNP) poles (Gordon, 1983). **B.** Paleolatitude values with 95% confidence intervals for the inclination groups. Also shown is the present-day latitude of the Hawaiian hotspot (black line). **C.** Estimated angular dispersion (S) of the inclination groups (black line) shown vs. the predicted values for 45-80 Ma (dark field) and 80-110 Ma (light field) from McFadden et al., (1991). **D.** Orthographic projection of the colatitude (primary) for Detroit seamount (star). The colatitude is distinct at the 99% confidence level (shaded) from previous 81-82 Ma poles (ellipses). Poles are derived from the following: 81 Ma (Gordon, 1983); 82 Ma (Sager and Pringle, 1988); 33n (79.1-73.6 Ma) (Vasas et al., 1994). The sense of offset between the NRM data and the demagnetized (primary) data is the same as that between the new paleolatitude result and results based on prior Pacific pole positions. This is the effect expected if these previous pole

positions are contaminated by secondary magnetizations. Figure is after Tarduno and Cottrell (1997). VGP = virtual geomagnetic pole.

Figure 6. Plot of latitudinal distance from the 43-Ma bend in the Hawaiian-Emperor hotspot track vs. age (light circles). Age data are not available for Meiji, Tenchi, and Jimmu; their positions, based on a constant latitudinal progression, are shown for reference. Dark gray circles indicate positions after the difference between the present-day latitude of the 43-Ma bend and Hawaii is subtracted from each of the present-day latitudes of the Emperor seamounts. In effect, we slide the Emperor trend down the Hawaiian chain so that the bend coincides with the position of Hawaii (inset). This reconstruction allows the following test. If the Emperor seamounts record mainly motion of the Hawaiian hotspot, paleolatitudes should fall close to this corrected latitudinal trend; if the hotspot has been stationary, the paleolatitudes should fall close to the present-day latitude of Hawaii. Triangles indicate the paleolatitudes of Suiko and Detroit Seamounts, with their 95% confidence intervals. The null hypothesis that the paleolatitude result from Suiko is drawn from the same population as the Detroit data can be rejected at the 95% confidence level using nonparametric tests (Kolmogorov - Smirnov). In the absence of a rotation of the entire solid Earth with respect to the spin axis, known as true polar wander (Tarduno and Cottrell, 1997; Cottrell and Tarduno, 2000b; Tarduno and Smirnov, 2001), the hotspot may have moved continuously southward at a rate of 30-50 mm/yr while the plate also drifted slowly northward (dark gray). Figure is after Tarduno and Cottrell (1997).

Figure 7. **A**. Estimates of zonal quadrupole Gauss coefficient (g_2^0) relative to the axial dipole (g_1^0) from Livermore et al. (1984). Pacific data are rotated using a fixed hotspot reference frame (see model "B" in Livermore et al., 1984). Our proposed sampling covers the range where Livermore et al. propose a change in sign of the quadrupole term. **B.** Paleointensity determined from studies of submarine basaltic glass (SBG) compiled by Juarez et al. (1998). The proposed sampling covers the transition from the Cretaceous Normal Polarity Superchron (K-N) to the Late Cretaceous-Cenozoic mixed polarity interval. VADM = virtual axial dipole moment.

Figure 8. Compositional changes in magmas produced by the Hawaiian hotspot through time. The shaded field shows the range of published $^{87}Sr/^{86}Sr$ of tholeiitic basalts vs. age and distance along the Hawaiian-Emperor chain. Note that data from Detroit seamount are significantly less radiogenic

than at younger volcanoes. The crossed circles connected by the thick dotted line shows the trend in age difference between seamounts and the underlying ocean crust (from Keller et al., 2000).

Figure 9. Proposed site locations (note change in scale): **(A)** Meiji Guyot, **(B)** Detroit Seamount, **(C)** Nintoku Seamount, **(D)** Ojin Seamount, and **(E)** Koko Guyot.

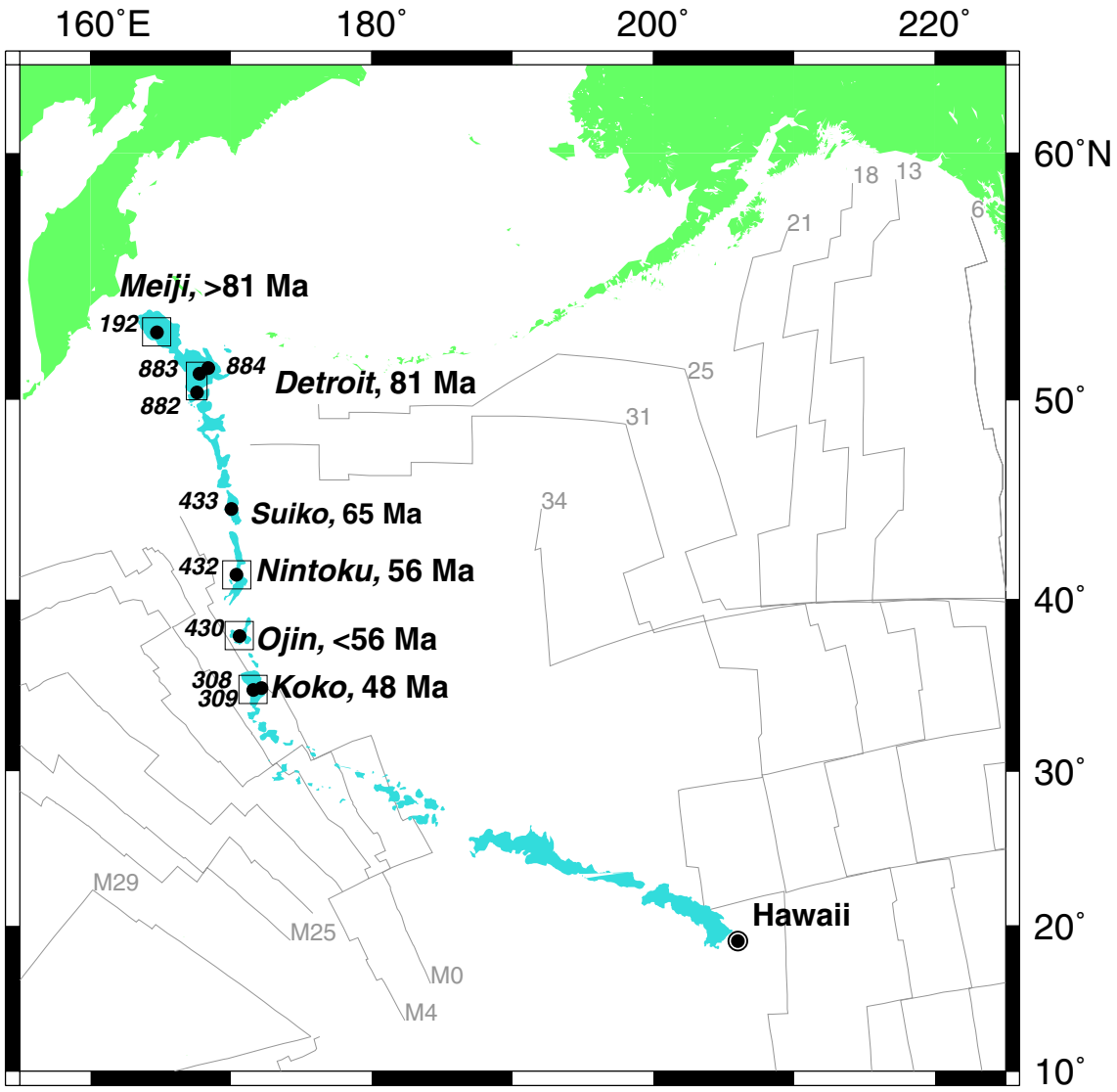
160˚E
180˚
200˚
220˚
60˚N
50˚
40˚
30˚
20˚
10˚
Meiji, >81 Ma
192
883
884
882
Detroit, 81 Ma
433
Suiko, 65 Ma
432
Nintoku, 56 Ma
430
Ojin, <56 Ma
308
309
Koko, 48 Ma
Hawaii
18
13
6
21
25
31
34
M29
M25
M0
M4

Figure 1

A

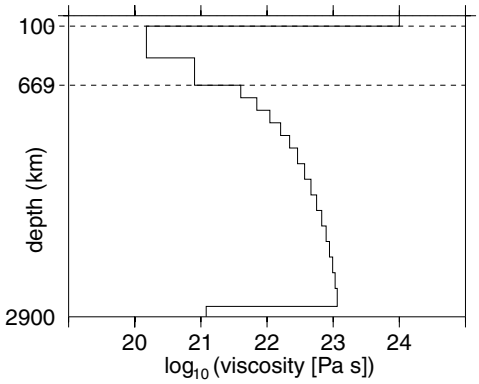
100
669
2900
depth (km)
20
21
22
23
24
log10 (viscosity [Pa s])

B

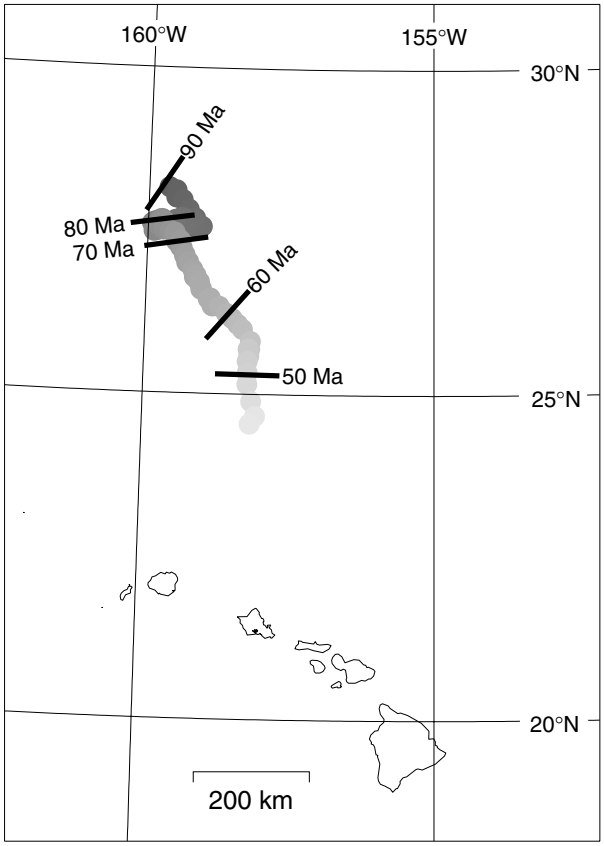
160°W
155°W
30°N
25°N
20°N
90 Ma
80 Ma
70 Ma
60 Ma
50 Ma
200 km

Figure 2

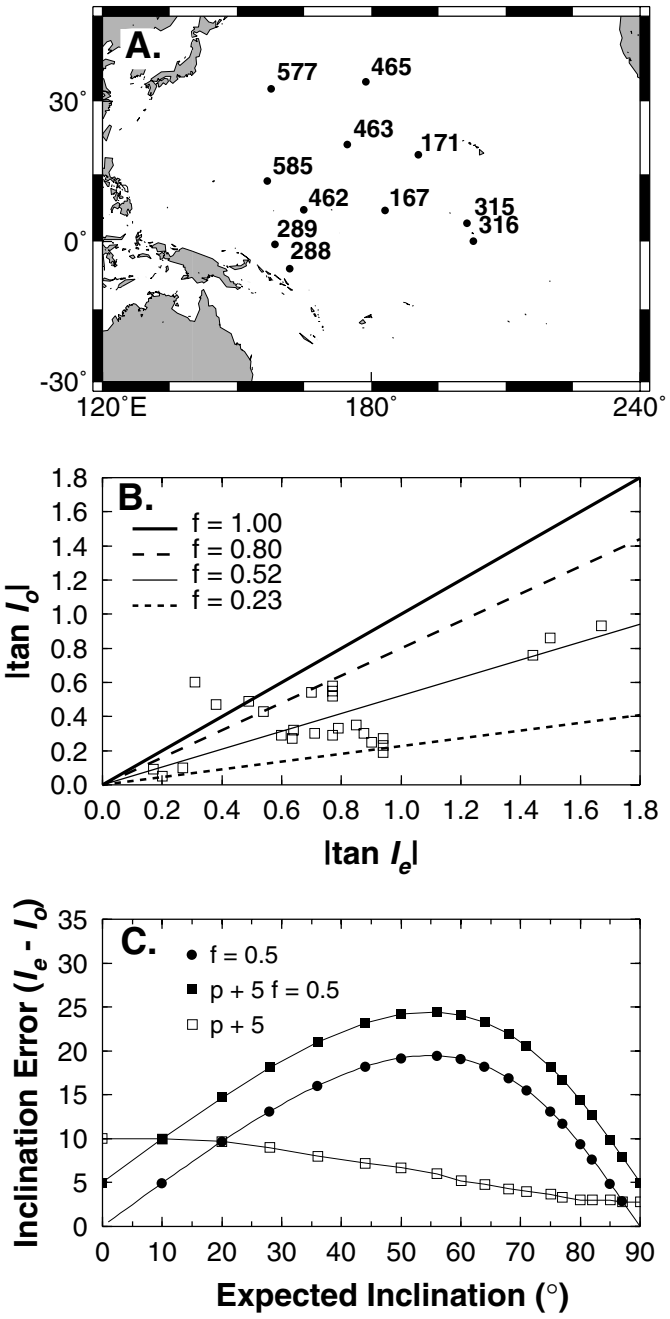
A.
577
465
463
171
585
462
167
315
316
289
288
30˚
0˚
-30˚
120˚E
180˚
240˚
B.
f = 1.00
f = 0.80
f = 0.52
f = 0.23
|tan I_o|
|tan I_e|
0.0 0.2 0.4 0.6 0.8 1.0 1.2 1.4 1.6 1.8
C.
f = 0.5
p + 5 f = 0.5
p + 5
Inclination Error (I_e - I_o)
Expected Inclination (°)
0 5 10 15 20 25 30 35
0 10 20 30 40 50 60 70 80 90

Figure 3

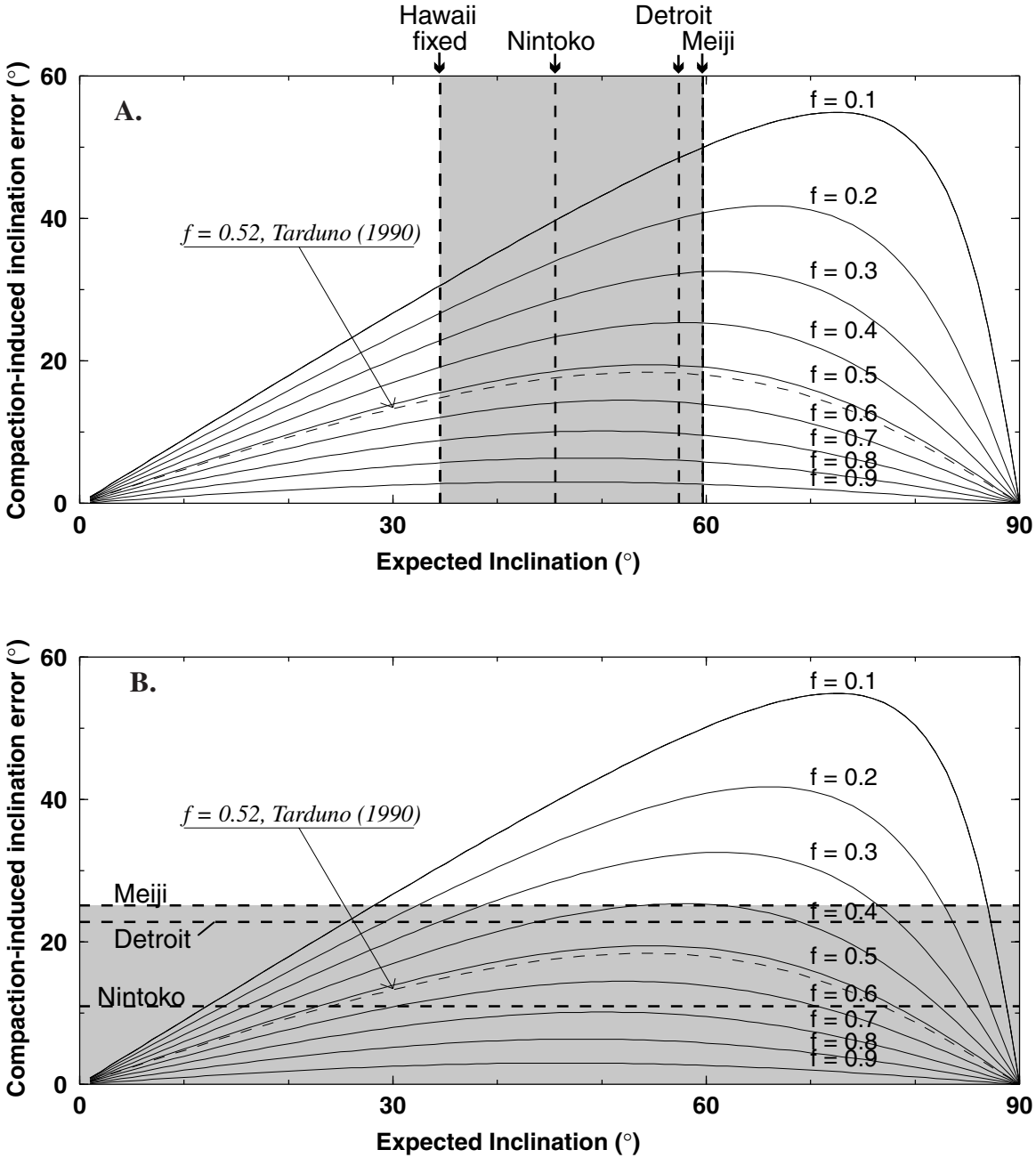
Hawaii fixed
Nintoko
Detroit
Meiji
A.
f = 0.52, Tarduno (1990)
f = 0.1
f = 0.2
f = 0.3
f = 0.4
f = 0.5
f = 0.6
f = 0.7
f = 0.8
f = 0.9
Compaction-induced inclination error (°)
Expected Inclination (°)
0
20
40
60
0
30
60
90
B.
Meiji
Detroit
Nintoko

Figure 4

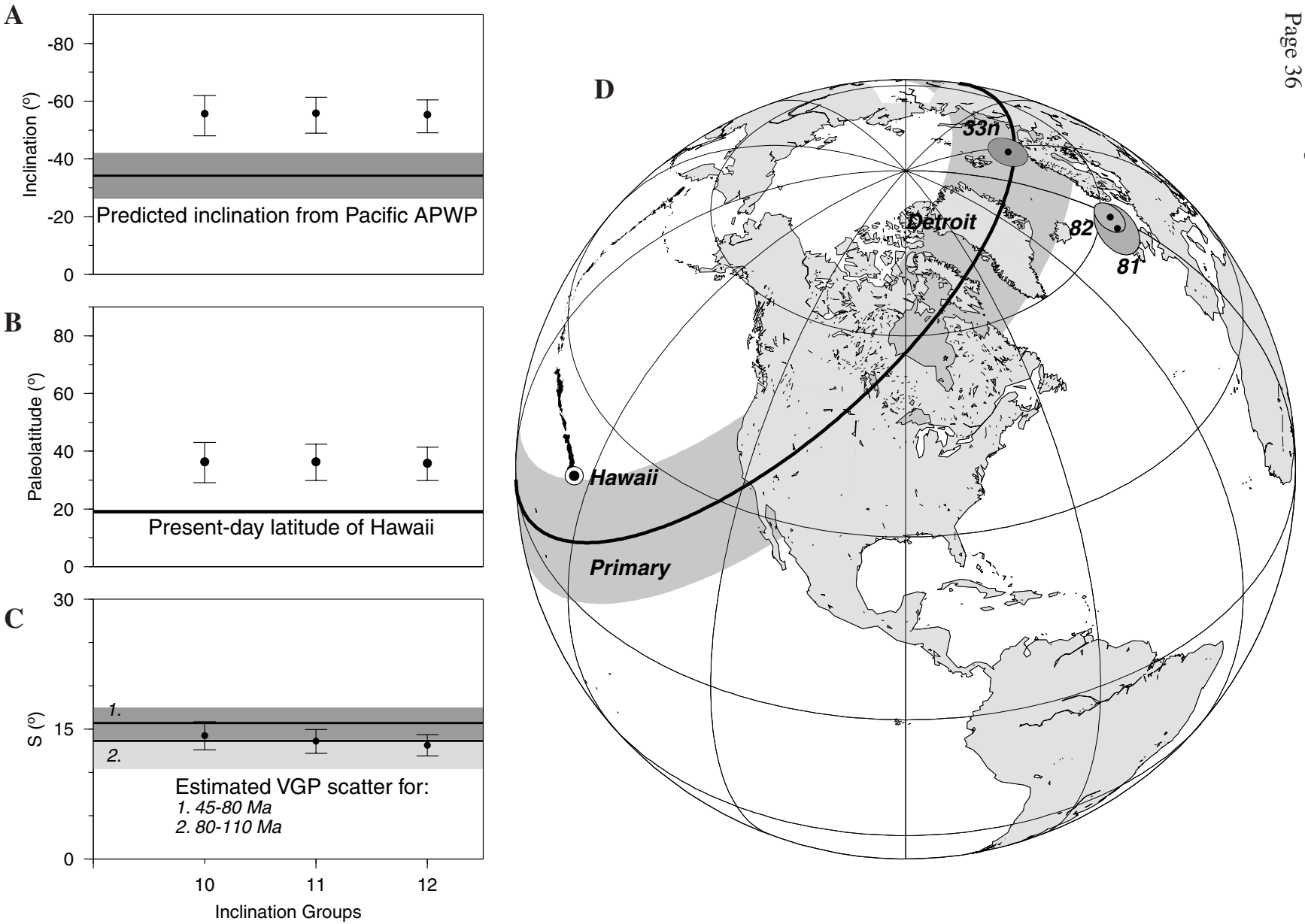
A
Inclination (°)
-80
-60
-40
-20
0
Predicted inclination from Pacific APWP
B
Paleolatitude (°)
80
60
40
20
0
Present-day latitude of Hawaii
C
S (°)
30
15
0
1.
2.
Estimated VGP scatter for:
1. 45-80 Ma
2. 80-110 Ma
10
11
12
Inclination Groups
D
33n
Detroit
82
81
Hawaii
Primary

Figure 5

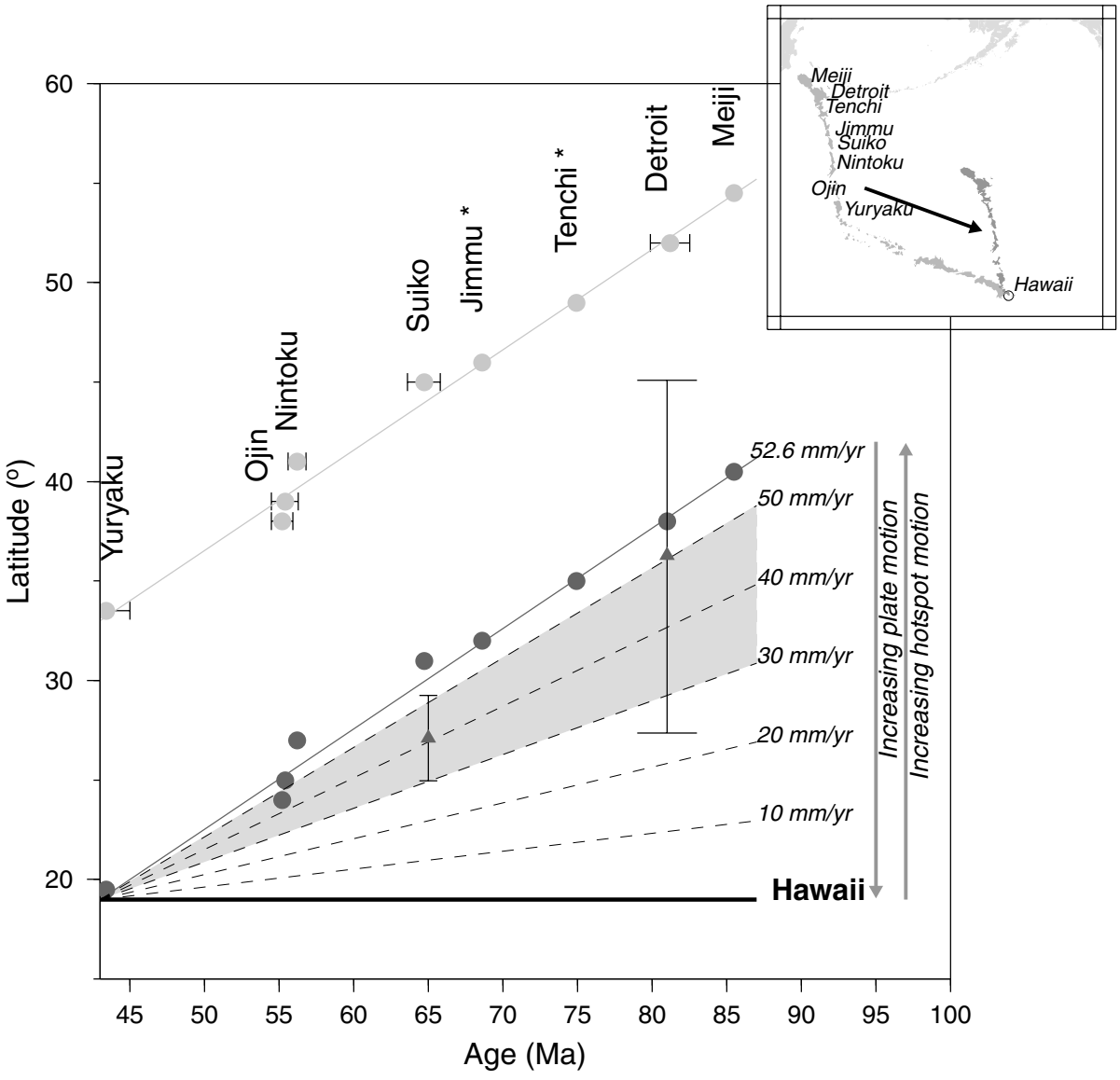
Latitude (°)
Age (Ma)
Yuryaku
Ojin
Nintoku
Suiko
Jimmu *
Tenchi *
Detroit
Meiji
52.6 mm/yr
50 mm/yr
40 mm/yr
30 mm/yr
20 mm/yr
10 mm/yr
Hawaii
Increasing plate motion
Increasing hotspot motion
Meiji
Detroit
Tenchi
Jimmu
Suiko
Nintoku
Ojin
Yuryaku
Hawaii

Figure 6

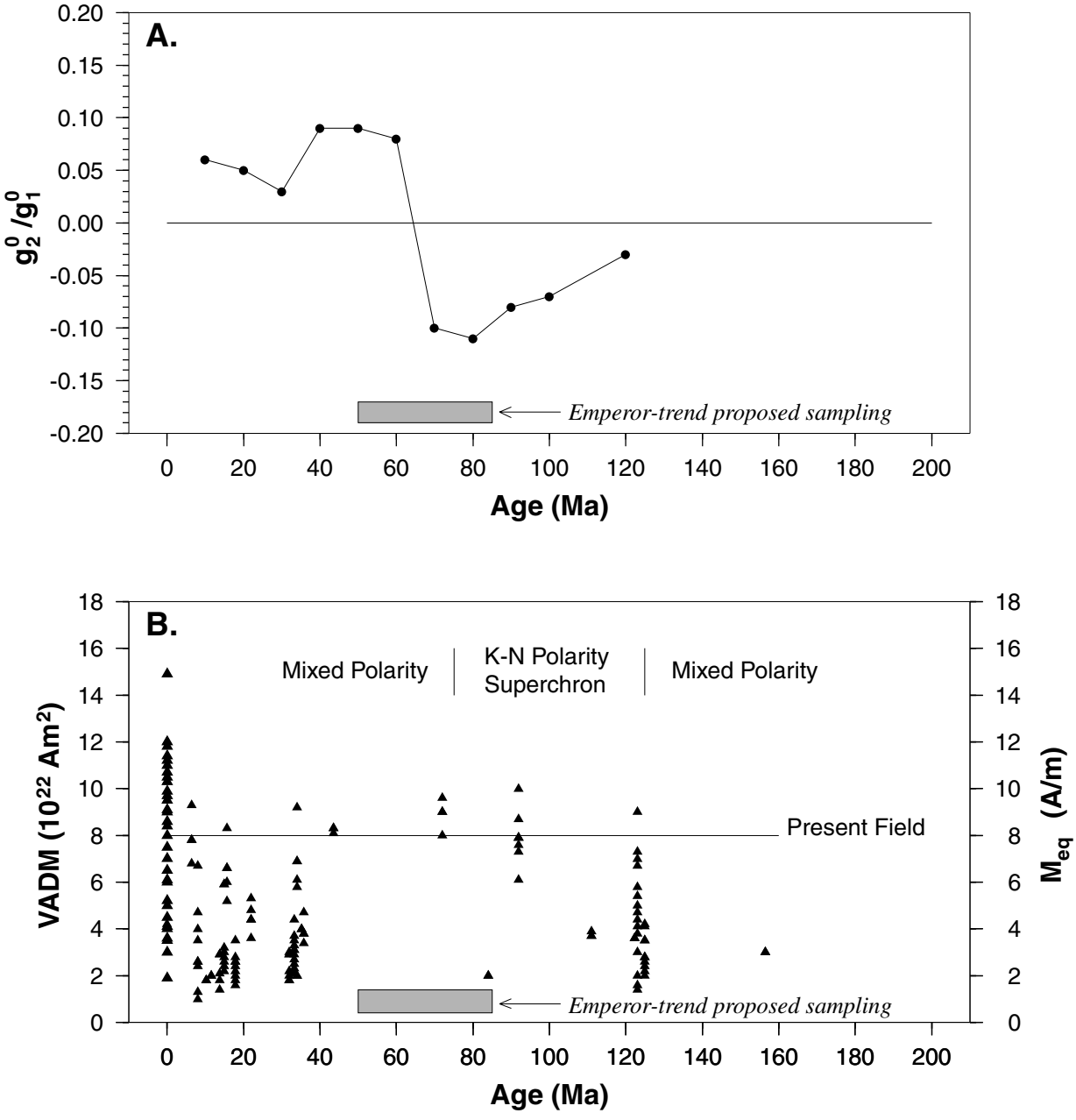
A.
g_2^0/g_1^0
Emperor-trend proposed sampling
Age (Ma)
B.
Mixed Polarity
K-N Polarity Superchron
Mixed Polarity
Present Field
VADM (10^{22} Am^2)
M_{eq} (A/m)
Emperor-trend proposed sampling
Age (Ma)

Figure 7

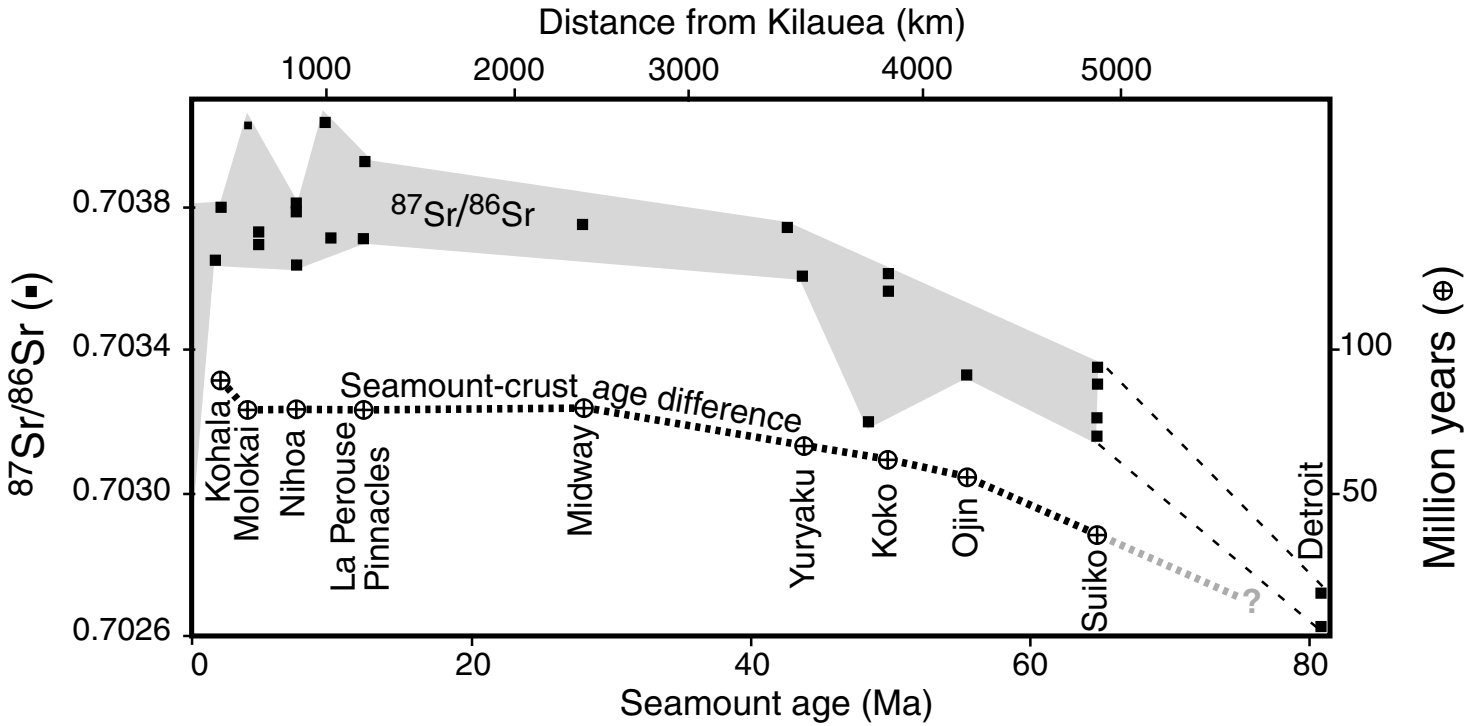
Distance from Kilauea (km)
1000
2000
3000
4000
5000
0.7038
0.7034
0.7030
0.7026
87Sr/86Sr (▪)
87Sr/86Sr
Seamount-crust age difference
Kohala
Molokai
Nihoa
La Perouse Pinnacles
Midway
Yuryaku
Koko
Ojin
Suiko
?
Detroit
100
50
Million years (⊕)
0
20
40
60
80
Seamount age (Ma)

Figure 8

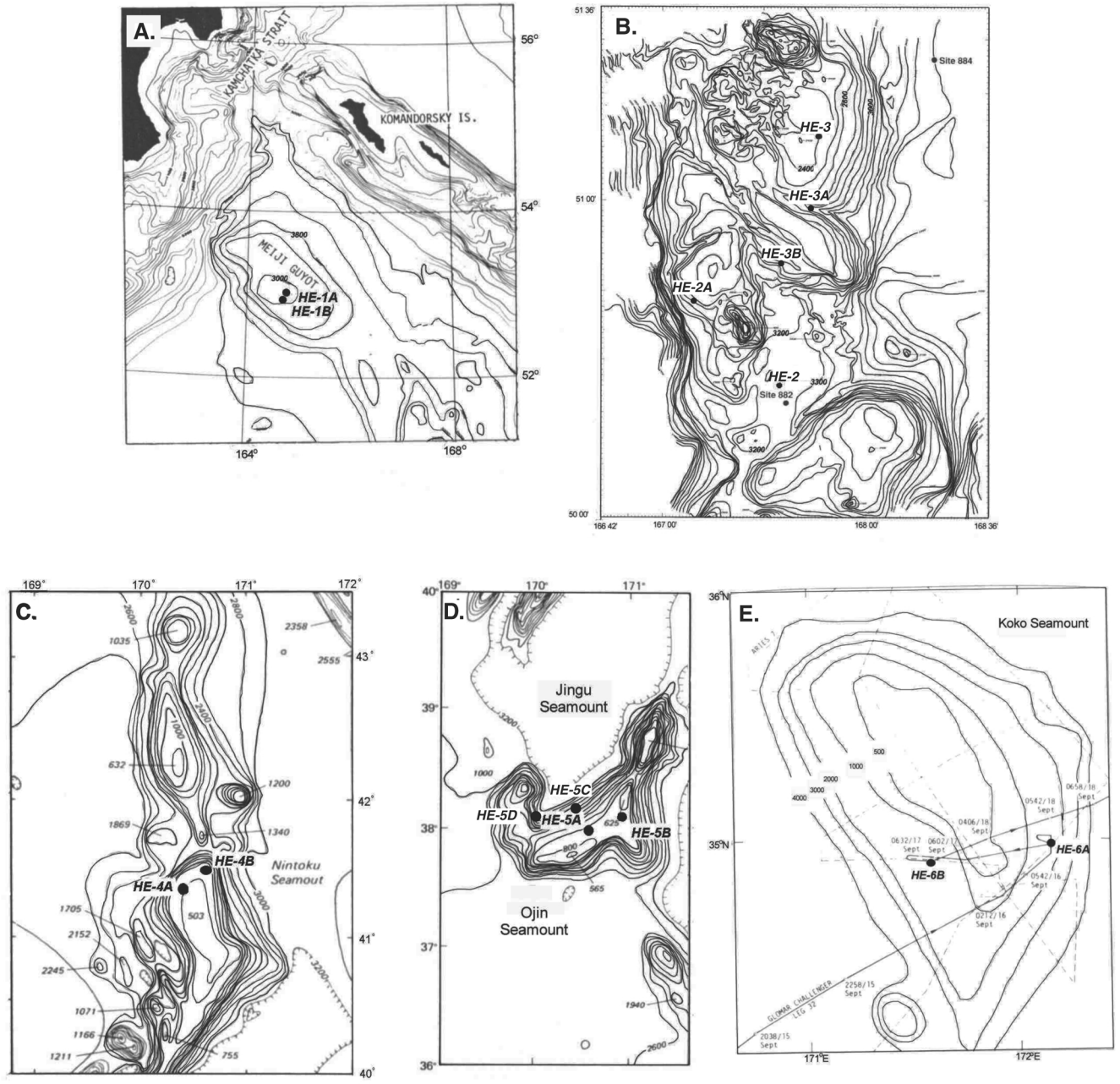
A.
KAMCHATKA STRAIT
KOMANDORSKY IS.
MEIJI GUYOT
HE-1A
HE-1B
56°
54°
52°
164°
168°
B.
Site 884
HE-3
HE-3A
HE-3B
HE-2A
HE-2
Site 882
51 36'
51 00'
50 00'
166 42'
167 00'
168 00'
168 36'
C.
Nintoku Seamount
HE-4A
HE-4B
43°
42°
41°
40°
D.
Jingu Seamount
HE-5C
HE-5D
HE-5A
HE-5B
Ojin Seamount
40°
39°
38°
37°
36°
E.
Koko Seamount
HE-6A
HE-6B
36°N
35°N
171°E
172°E

Figure 9

Leg 197 Operations Plan and Time Estimate

Option 1

Site No.	Location Lat/Long	Water Depth	Operations Description	Transit (days)	Drilling (days)	Logging (days)	Total On-site
		(mbrf)					
Yokohama	35°16.80'N		Transit 1572 nmi from Yokohama, Japan to Site HE-1B @ 11.0 kt	6.0			
	139°23.40'E						
HE-1B	52°53.00'N	3200	Drill ahead with a center bit to 800 mbsf.		9.6	0.9	10.5
	164°35.00'E		RCB in sediment from 800 to 950 mbsf				
			Wireline logs (Triple combo and FMS)				
			Transit 167 nmi from Site HE-1B to Site HE-3B @ 11.0 kt	0.6			
HE-3B	50°48.60'N	2740	Drill ahead through sediment with a center bit to 450 mbsf		7.1	1.1	8.2
	167°33.00'E		RCB from 450 to 600 mbsf (150 m into basement) using FFF				
			for one bit change				
			Wireline logs (Triple combo, Mag Tool, and FMS)				
			Transit 574 nmi from Site HE-3B to Site HE-4B @ 10.5 kt	2.3			
HE-4B	41°29.00'N	1300	RCB to 190 mbsf (150 m into basement)		4.8	0.5	5.3
	170°38.00'E		Wireline logs (Triple combo and FMS)				
			Transit 200 nmi from Site HE-4B to Site HE-5C @ 10.5 kt	0.8			
HE-5C	38°09.50'N	1480	RCB to 210 mbsf (150 m into basement)		4.9	0.5	5.4
	170°50.00'E		Wireline logs (Triple combo and FMS)				
			Transit 201 nmi from Site HE-5C to Site HE-6A @ 10.5 kt	0.8			
HE-6A	34°58.94'N	1331	RCB to 230 mbsf (150 m into basement)		4.8	0.5	5.3
	172°08.98'E		Wireline logs (Triple combo and FMS)				
Yokohama	35°16.80'N		Transit 1640 nmi from Site HE-6A to Yokohama, Japan @ 10.0 kt	6.8			
	139°23.40'E						
			TOTAL:	**17.3**	**31.2**	**3.5**	**34.7**

TOTAL DAYS: 52.0

Leg 197 Operations Plan and Time Estimate

Option 2

Site No.	Location Lat/Long	Water Depth	Operations Description	Transit (days)	Drilling (days)	Logging (days)	Total On-site
		(mbrf)					
Yokohama	35°16.80'N		Transit 1552 nmi from Yokohama, Japan, to Site HE-3B @ 11.0 kt	5.9			
	139° 23.40' E						
HE-3B	50° 48.60' N	2740	Drill ahead through sediment with a center bit to 450 mbsf		7.6	1.3	8.9
	167° 33.00' E		RCB from 450 to 620 mbsf (170 m into basement) using				
			FFF for one bit change				
			Wireline logs (Triple combo, Mag Tool, and FMS)				
			Transit 11 nmi from Site HE-3B to Site HE-3A @ 11.0 kt	0.0			
HE-3A	50° 57.00' N	2773	Drill ahead through sediment with a center bit to 500 mbsf		7.5	0.9	8.4
	167° 44.40' E		RCB from 500 to 670 mbsf (170 m into basement) using FFF				
			for one bit change				
			Wireline logs (Triple combo and FMS)				
			Transit 580 nmi from Site HE-3A to Site HE-4B @ 10.5 kt	2.3			
HE-4B	41° 29.00' N	1300	RCB to 220 mbsf (180 m into basement)		5.4	0.6	6.0
	170° 38.00' E		Wireline logs (Triple combo and FMS)				
			Transit 200 nmi from Site HE-4B to Site HE-5C @ 10.5 kt	0.8			
HE-5C	38° 09.50' N	1480	RCB to 240 mbsf (180 m into basement)		5.6	0.6	6.2
	170° 50.00' E		Wireline logs (Triple combo and FMS)				
			Transit 201 nmi from Site HE-5C to Site HE-6A @ 10.5 kt	0.8			
HE-6A	34° 58.94' N	1331	RCB to 260 mbsf (180 m into basement)		5.4	0.6	6.0
	172° 08.98' E		Wireline logs (Triple combo and FMS)				
Yokohama	35° 16.80' N		Transit 1640 nmi from Site HE-6A to Yokohama, Japan @ 10.0 kt	6.8			
	139° 23.40' E						
			TOTAL:	**16.5**	**31.5**	**4.0**	**35.5**

TOTAL DAYS: 52.0

Leg 197 Operations Plan and Time Estimate

Option 3

Site No.	Location Lat/Long	Water Depth	Operations Description	Transit (days)	Drilling (days)	Logging (days)	Total On-site
		(mbrf)					
Yokohama	35°16.80'N		Transit 1552 nmi from Yokohama, Japan, to Site HE-3B @ 11.0 kt	5.9			
	139°23.40'E						
HE-3B	50°48.60'N	2740	Drill ahead through sediment with a center bit to 300 mbsf		8.1	1.2	9.3
	167°33.00'E		RCB in sediment from 300 to 450 mbsf				
			RCB from 450 to 600 mbsf (150 m into basement) using				
			FFF for one bit change				
			Wireline logs (Triple combo, Mag Tool, and FMS)				
			Transit 11 nmi from Site HE-3B to Site HE-3A @ 11.0 kt	0.0			
HE-3A	50°57.00'N	2773	Drill ahead through sediment with a center bit to 300 mbsf		8.2	0.8	9.0
	167°44.40'E		RCB in sediment from 300 to 500 mbsf				
			RCB from 500 to 650 mbsf (150 m into basement) using				
			FFF for one bit change				
			Wireline logs (Triple combo and FMS)				
			Transit 580 nmi from Site HE-3A to Site HE-4B @ 10.5 kt	2.3			
HE-4B	41°29.00'N	1300	RCB to 200 mbsf (160 m into basement)		5.1	0.6	5.7
	170°38.00'E		Wireline logs (Triple combo and FMS)				
			Transit 200 nmi from Site HE-4B to Site HE-5C @ 10.5 kt	0.8			
HE-5C	38°09.50'N	1480	RCB to 220 mbsf (160 m into basement)		5.3	0.6	5.9
	170°50.00'E		Wireline logs (Triple combo and FMS)				
			Transit 201 nmi from Site HE-5C to Site HE-6A @ 10.5 kt	0.8			
HE-6A	34°58.94'N	1331	RCB to 240 mbsf (160 m into basement)		5.0	0.6	5.6
	172°08.98'E		Wireline logs (Triple combo and FMS)				
Yokohama	35°16.80'N		Transit 1640 nmi from Site HE-6A to Yokohama, Japan @ 10.0 kt	6.8			
	139°23.40'E						
			TOTAL:	**16.5**	**31.7**	**3.8**	**35.5**

TOTAL DAYS: 52.0